

Signed Diverse Multiplex Networks: Clustering and Inference

Marianna Pensky, University of Central Florida

Abstract—The paper introduces a Signed Generalized Random Dot Product Graph (SGRDPG) model, which is a variant of the Generalized Random Dot Product Graph (GRDPG), where, in addition, edges can be positive or negative. The setting is extended to a multiplex version, where all layers have the same collection of nodes and follow the SGRDPG. The only common feature of the layers of the network is that they can be partitioned into groups with common subspace structures, while otherwise matrices of connection probabilities can be all different. The setting above is extremely flexible and includes a variety of existing multiplex network models, including GRDPG, as its particular cases. By employing novel methodologies, our paper ensures strongly consistent clustering of layers and highly accurate subspace estimation, which are significant improvements over the results of Pensky and Wang (2024). All algorithms and theoretical results in the paper remain true for both signed and binary networks. In addition, the paper shows that keeping signs of the edges in the process of network construction leads to a better precision of estimation and clustering and, hence, is beneficial for tackling real world problems such as, for example, analysis of brain networks.

Index Terms—Multiplex Network, clustering, Generalized Random Dot Product Graph

I. INTRODUCTION

A. Signed Generalized Random Dot Product Graph (SGRDPG) model

Stochastic network models appear in a variety of applications, including genetics, proteomics, medical imaging, international relationships, brain science and many more. In the last few decades, researchers developed a variety of ways to model those networks, imposing some restriction on the matrix of probabilities that generates random edges. The block models and the latent position graph settings are perhaps the most popular ways of modeling random graphs. In particular, the Generalized Random Dot Product Graph (GRDPG) model is a latent position graph model which has great flexibility. However, the GRDPG requires assumptions that are difficult to satisfy. In order to remove this shortcoming, below we introduce the Signed Generalized Random Dot Product Graph (SGRDPG) model and extend it to a multilayer setting.

Consider a undirected network with n nodes and without self-loops. The GRDPG model refers to a network where the matrix of connection probabilities is of the form

$$P = UQU^T, \quad Q = Q^T \in \mathbb{R}^{K \times K}. \quad (1)$$

Here $U \in \mathbb{R}^{n \times K}$ is a matrix with orthonormal columns, and U and Q are such that all entries of P are in $[0, 1]$. The

GRDPG network model is very flexible and is known to have a variety of the network models as its particular cases: the Stochastic Block Model (SBM), the Degree Corrected Block Model ([20]), the Popularity Adjusted Block Model ([29], [34]), the Mixed Membership Model (MMM) ([3], [10]), or the Degree Corrected Mixed Membership Model ([27]). If all eigenvalues of matrix Q are positive, then model (1) reduces to the Random Dot Product Graph (RDPG) model (see, e.g., the survey in [5]). The RDPG and the GRDPG models ([5], [38]) have recently gained an increasing popularity.

Nevertheless, the condition that elements of matrix P in (1) are indeed probabilities is not easy to satisfy. Indeed, unless a network is generated using one of the above mentioned block model scenarios and matrices U and Q are found later by using the Singular Value Decomposition (SVD), it is very difficult to guarantee that the elements of matrix P are nonnegative. The latter is due to the fact that, in general, elements of matrix U can be positive or negative. To the best of our knowledge, the only papers that study conditions for the elements of matrix P to be non-negative, are [23] and its sequel [24]. While these papers provide some sufficient conditions for non-negativity, these conditions are far from trivial, and it is not clear how to satisfy them in a generic setting. In addition, [24] and the second half of [23] focus on the case where the first (positive) eigenvalue is significantly larger than the rest of the singular values combined. This is the opposite scenario from the majority of GRDPG studies where, similarly to our paper, it is assumed that all singular values are of the same order of magnitude. In summary, imposing conditions that ensure non-negativity is far from trivial and, for this reason, all simulation studies for the GRDPG always consider one of the existing block models, e.g., SBM or MMM.

To eliminate this difficulty and to add further flexibility to the model, here we propose the Signed Generalized Dot Product Graph (SGRDPG) model which generates an edge between nodes i and j with probability $|P_{i,j}|$ and the corresponding element of the adjacency matrix $A(i, j)$ can be zero, 1 or -1:

$$\begin{aligned} \mathbb{P}(|A(i, j)| = 1) &= |P(i, j)|, \quad \text{sign}(A(i, j)) = \text{sign}(P(i, j)), \\ A(i, j) &= A(i, j) \quad 1 \leq i < j \leq n \end{aligned} \quad (2)$$

It is easy to ensure that $|P(i, j)| \leq 1$ since the latter is guaranteed by the row norms of matrix U being bounded by one and the eigenvalues of matrix Q being in the interval $[-1, 1]$. Observe that, if elements of matrix P are nonnegative, the SGRDPG immediately reduces to the existing GRDPG model. The setting (2) can also be viewed as a particular case

of a Weighted Graph introduced in [18]. However, the Signed GRDPG model does not require special tools for its analysis, unlike the Weighted Graph model in [18], and also can be easily extended to a multilayer context.

Note that the model above is motivated by situations where signs of edges are present but are not associated with any intrinsic patterns. For example, biological networks are often constructed on the basis of correlation (or precision) matrices, elements of which can be positive or negative. It often happens that, when data of this sort are modeled by a network, the signs of the edges are removed which leads to a significant loss of accuracy. We should mention that SGRDPG may not be a suitable tool to model social networks where relation between two nodes can be positive ("friendship"), or negative ("animosity"), or zero ("no relationship"), and the distribution of signs is strongly associated with the structure of probability matrix. For example, modeling of social networks is often restricted by the so called balance theory which puts restrictions on the signs of the edges. In particular, the maxims "an enemy of my enemy is my friend" and "two of my friends cannot be enemies" lead to the fact that any closed triangle in a signed network can have either two or zero negative edges (strong balance). The allure of the strong balance formulation lies in the fact that strongly balanced networks are clusterable ([22]), i.e., the nodes can be divided into some number of disjoint sets such that all edges within sets are positive and all edges between sets are negative. This is, however, a sufficient condition while the necessary condition for clusterability is the so called weak balance ([13]), which requires that there are no closed loops in the network with exactly one negative edge. However, many of the existing real world networks are not balanced. This particularly applies to biological networks, where there is no intrinsic reason for the balance.

Therefore, in this paper we do not associate the signs distribution with any intrinsic pattern, as it is done in, e.g., [12], and instead just preserve the sign of each edge, while modeling the probabilities of connections using the most flexible GRDPG model.

B. DIMPLE-SGRDPG: the SGRDPG-equipped Diverse Multiplex network

While in the early years of the field of stochastic networks, research mainly focused on studying a single network, in recent years the frontier moved to investigation of collection of networks, the so called *multilayer network*, which allows to study relationships between nodes with respect to various modalities (e.g., relationships between species based on food or space), or consists of network data collected from different individuals (e.g., brain networks). Although there are many different ways of modeling a multilayer network (see, e.g., an excellent review article of [28]), in this paper, we consider a *Multiplex Network Model* where all layers have the same set of nodes, and all the edges between nodes are drawn within layers, i.e., there are no edges connecting the nodes in different layers. Multiplex network models have a variety of applications such as brain networks ([39]) where nodes are brain regions and layers are individuals, or trade networks

([14]) where nodes and layers represent, respectively, various countries and commodities in which they are trading.

Many authors researched multiplex network models, imposing an array of restrictions of varying degree of severity. The simplest of the multiplex network models, the "checker board model" of [11], assumes that all layers are equipped with the Stochastic Block Models, all layers have the same communities and there are only few distinct block connectivity matrices. On the other hand, the DIVERse MultiPLEx Generalized Random Dot Product Graph (**DIMPLE-GRDPG**) in [37] considers layers that follow the GRDPG model ([38]) and allows utmost variability in layers' structures and connectivity patterns throughout the network.

The present paper follows this most general multiplex network model of [37], and, in addition, allows edges to be equipped with signs. The objective of the paper is twofold. First, it demonstrates that, even for this extremely complex multilayer network, one can achieve **similar or better inference precision**, than has been obtained for simpler multiplex network models. Second, it shows that keeping signs of the edges in the process of network construction leads to a more accurate estimation and clustering.

Specifically, this paper studies a multiplex network where each layer follows the SGRDPG model introduced in (2). Consider an L -layer network on the same set of n vertices $[n] := \{1, \dots, n\}$. The tensor of connection probabilities $\mathbf{P} \in [0, 1]^{n \times n \times L}$ is formed by layers $P^{(l)}$, $l \in [L]$, which can be partitioned into M groups, so that there exists a label function $s : [L] \rightarrow [M]$. It is assumed that the probability matrices $P^{(l)}$ of the layers of the network follow the SGRDPG model defined in (1) and (2), and that each group of layers is embedded in its own ambient subspace, but otherwise all matrices of connection probabilities can be different. In particular, $P^{(l)}$, $l \in [L]$, are given by

$$P^{(l)} = U^{(m)} Q^{(l)} (U^{(m)})^T, \quad m = s(l), \quad (3)$$

where $Q^{(l)} = (Q^{(l)})^T$, and $U^{(m)}$, $m \in [M]$, are matrices with orthonormal columns. Here, however, matrices $U^{(m)}$ and $Q^{(l)}$ are not required to ensure that elements of matrices $P^{(l)}$ are probabilities, but just that they lie in the interval $[-1, 1]$, which is a much easier condition to satisfy. We shall call this setting the DIVERse MultiPLEx Signed Generalized Random Dot Product Graph (**DIMPLE-SGRDPG**).

Here, one observes the adjacency tensor $\mathbf{A} \in \{0, 1, -1\}^{n \times n \times L}$ with layers $A^{(l)}$ such that $A^{(l)}(i, j)$ are independent from each other for $1 \leq i < j \leq n$ and $l \in [L]$, $A^{(l)}(i, j) = A^{(l)}(j, i)$. and follow (2), i.e.,

$$\begin{aligned} \mathbb{P}(|A^{(l)}(i, j)| = 1) &= |P^{(l)}(i, j)|, \\ \text{sign}(A^{(l)}(i, j)) &= \text{sign}(P^{(l)}(i, j)) \end{aligned} \quad (4)$$

The objective is to recover the between-layer clustering function $s : [L] \rightarrow [M]$ with the corresponding clustering matrix S , and the bases $U^{(m)}$ of the ambient subspaces in (3). Note that, however, the main task in the DIMPLE-SGRDPG model is the between-layer clustering. If the groups of layers are correctly identified, then the layers with common subspace structures can be pooled together in a variety of ways, as it is done in [4] or [37].

Introduction of a model, where groups of layers can be embedded into different subspaces, is undeniably very crucial. Indeed, after embedding layers of a network into an appropriate subspace, further inference usually relies on asymptotic normality of estimators of matrices $Q^{(l)}$, which, in turn, requires that the ratios between the highest and the lowest eigenvalues of matrices $Q^{(l)}$ are bounded above. However, this is not true if a network follows model (3), where matrices $U^{(m)}$ represent different subspaces, but are modeled using only one common subspace U . As it is easy to see, matrix U will have higher rank than matrices $U^{(m)}$, so that the lowest eigenvalues of all matrices $Q^{(l)}$ will be equal to zero.

Nevertheless, in this paper, we are not interested in estimating the matrices $Q^{(l)}$ in (3) since they act as nuisance parameters, as far as the inference on the structure of the network is concerned. If desired, those matrices can be recovered by standard methods (see, e.g., [5]).

C. Existing results and technical challenges

The DIMPLE-SGRDPG model is a relatively straightforward extension of the DIMPLE-GRDPG model of [37], which, in turn, generalizes a multitude of multiplex network models.

In particular, if all layers share the same ambient subspace structure, i.e., $M = 1$ in (3), the DIMPLE-GRDPG reduces to the COSIE model in [4] and [46]. Furthermore, there is a multitude of papers that study SBM-equipped multiplex networks, which constitute particular cases of the DIMPLE-GRDPG (see an extensive discussion in [35] and references therein). Moreover, the multiplex network equipped with the Degree-Corrected Stochastic Block Models, featured in [1], also reduces to the COSIE model with $M = 1$, due to the fact that the positions of the diagonal weight matrices and the membership matrices can be interchanged in the presentation of the layer probability matrices.

Furthermore, we should comment on the relationship of the DIMPLE-SGRDPG model to the low-rank tensor models. In those models, one can represent a low rank tensor using the Tucker decomposition with a low-dimensional core tensor and subsequently recover the subspaces and the core tensor using the Higher Order Orthogonal Iterations (**HOOI**) (see, e.g., [2], [21], [33], [45]). The papers cited above, however, assume the noise components to be Gaussian (or sub-Gaussian with particular parameters) which makes their results not transferable to sparse binary networks. Recently, [17] and [25] considered the Mixed MultiLayer Stochastic Block Model (**MMLSBM**), where the layers can be partitioned into M groups, with each group of layers equipped with its unique SBM. The MMLSBM is a particular case of the DIMPLE-GRDPG in (3), where $Q^{(l)} \equiv Q^{(m)}$, $l \in [L]$, depend on $m = s(l)$ only.

Note that in all the papers cited above, the probability tensor \mathbf{P} is of low rank, with the subspace structures associated with the problems of interest, and the inference relies on application of HOOI (except in [17] which uses an Alternating Minimization Algorithm). Nonetheless, our framework is not generated by a low rank tensor. Instead, (3) and (4) can be viewed as a signed binary tensor which, in expectation, due to

matrices $Q^{(l)}$ being arbitrary, reduces to a partial multilinear structure as in, e.g., Section 5 of [33]. In this case, one can recover the subspaces associated with the low-rank modes with much better precision than the high-rank mode which, in our case, is associated with the network layer clustering.

However, so far it appeared that the flexibility of the DIMPLE-SGRDPG network comes at a price. Indeed, if ρ_n is the sparsity parameter of network, so that $\max_{i,j,l} |P^{(l)}(i,j)| \geq C\rho_n \geq Cn^{-1} \log n$, then [37] show that the proportion of mis-clustered layers is bounded above by $C(n\rho_n)^{-1}$ and, unfortunately, the between-layer clustering error dominates the error of estimating of matrices $U^{(m)}$ in (3), or community detection in groups of layers when the layers of the network are equipped with the SBMs.

The goal of the present paper is to eliminate this deficiency, and to develop a strongly consistent between-layer clustering algorithm that leads to the same errors of subspaces recoveries that are obtained in simpler models like COSIE. The latter is achieved by removing the common components from subspaces and employing the $\ell_{2,\infty}$ -norm based evaluations. The new technique delivers strongly consistent between-layer clustering under assumptions that are very similar to the ones in [37]. The latter guarantees highly accurate estimators of the subspace basis matrices $U^{(m)}$, or community assignments in groups of layers, for a SBM-equipped multiples network. The specific error rates are thoroughly discussed in Remarks 5 and 7 in Section III.

We should mention that all algorithms and theoretical assessments in the paper remain correct for un-signed multiplex networks with binary adjacency matrices. Nevertheless, as simulations and real data examples show, an opportunity of retaining signs of edges when they are present allows to achieve better clustering precision.

Remark 1. Relation to time-varying networks. The DIMPLE-GRDPG can also be viewed as a generalization of a time-varying network with the GRDPG-equipped layers (e.g., [6]). However, the inference in a multiplex network is much more difficult than in the respective dynamic network since, in a dynamic network, the layers are ordered according to time instances, while in a multiplex network the enumeration of layers is completely arbitrary. The latter makes techniques designed for dynamic networks unsuitable for the inference in the DIMPLE-GRDPG setting.

D. Our contributions

Our paper makes several key contributions.

- 1) To the best of our knowledge, our paper is the first one to introduce the very flexible signed SGRDPG network model and to extend it to the multilayer case. The difference between our SGRDPG model and other signed network settings is that it immediately reduces to GRDPG when no signs are present, and hence provides a true generalization of the popular GRDPG model. Hence, we are considering the most broad case of the multiplex networks with latent position/block model equipped layers.

- 2) Our paper offers a novel **strongly consistent** between-layer clustering algorithm that works for the GRDPG and SGRDPG equipped multiplex networks, when the sparsity ρ_n satisfies $n\rho_n \geq C \log n$. This result has been previously achieved only in much simpler multiplex network models, where layers are equipped with the SBMs (see [35]).
- 3) Our paper develops novel theoretical results under very simple and intuitive assumptions. First, it establishes theoretical guarantees for the strongly consistent between-layer clustering for the new very general model. In addition, it provides upper bounds on the subspace estimation errors in both operator and $(2, \infty)$ norms. While the former are derived by techniques similar to those, employed in [37], the latter employ novel ideas and are **significantly better** than the rates obtained in [46] for the simpler COSIE model. All results in the paper remain valid for “un-signed” multiplex networks with binary adjacency matrices.
- 4) Simulations in the paper establish that the between-layer and the within-layer clustering algorithms deliver high precision in a finite parameter settings. In addition, simulations and real data example confirm that, in the case when edges of the network can naturally be positive or negative, keeping signs of the edges in the process of network construction leads to better accuracy of estimation and clustering, and, hence, is beneficial for tackling real world problems such as analysis of brain networks.
- 5) Since our setting includes majority of the popular network models as its particular cases, our approach removes the need for testing, which of the particular network models should be used for the layers. After the groups of layers with similar ambient subspace structures are identified, one can recover those common structures and subsequently estimate community assignments, if one suspects that a block model generated networks in the layers.

E. Notations and organization of the paper

We denote $a_n = O(b_n)$ if $a_n \leq Cb_n$, $a_n = \omega(b_n)$ if $a_n \geq cb_n$, $a_n \propto b_n$ if $cb_n \leq a_n \leq Cb_n$, where $0 < c \leq C < \infty$ are absolute constants independent of n . Also, $a_n = o(b_n)$ and $a_n = \Omega(b_n)$ if, respectively, $a_n/b_n \rightarrow 0$ and $a_n/b_n \rightarrow \infty$ as $n \rightarrow \infty$. We use C as a generic absolute constant independent of n, L, M and K .

For any vector $v \in \mathbb{R}^p$, denote its ℓ_2 , ℓ_1 , ℓ_0 and ℓ_∞ norms by $\|v\|$, $\|v\|_1$, $\|v\|_0$ and $\|v\|_\infty$, respectively. Denote by 1_m the m -dimensional column vector with all components equal to one.

For any matrix A , denote its spectral, Frobenius and $(2, \infty)$ norms by, respectively, $\|A\|$, $\|A\|_F$, $\|A\|_{2,\infty} = \max \|A(i, :)\|$ and $\|A\|_{1,\infty} = \max \|A(i, :)\|_1$. Denote the eigenvalues and singular values of A by $\lambda(A)$ and $\sigma(A)$, respectively. Let $\text{SVD}_r(A)$ be r left leading eigenvectors of A . The column j and the row i of a matrix A are denoted by $A(:, j)$ and $A(i, :)$, respectively. Let $\text{vec}(A)$ be the vector obtained from

matrix A by sequentially stacking its columns. Denote by $A \otimes B$ the Kronecker product of matrices A and B . Denote the diagonal of a matrix A by $\text{diag}(A)$. Also, with some abuse of notations, denote the K -dimensional diagonal matrix with a_1, \dots, a_K on the diagonal by $\text{diag}(a_1, \dots, a_K)$, and the diagonal matrix consisting of only the diagonal of a square matrix A by $\text{diag}(A)$. Denote $\mathcal{O}_{n,K} = \{A \in \mathbb{R}^{n \times K} : A^T A = I_K\}$, $\mathcal{O}_n = \mathcal{O}_{n,n}$. Denote by $\mathcal{C}_{n,K}$ the set of clustering matrices $X \in \{0, 1\}^{n \times K}$ that partition n objects into K clusters, where X is a clustering matrix if it is binary and has exactly one 1 per row. Also, we denote an absolute constants independent of n, K, L and M , which can take different values at different instances, by C .

The rest of the paper is organized as follows. Section II introduces a natural generative mechanism for a network that follows the DIMPLE-SGRDPG model and presents algorithms for its analysis. Specifically, Section II-C suggests a novel between-layer clustering algorithm, while Section II-D examines techniques for fitting subspaces in groups of layers. Section III provides theoretical guarantees for the methodologies in Section II: the upper bounds on the between-layer clustering errors (Section III-B), the subspace fitting errors (Section III-C), and the errors in the special case of the Stochastic Block Model and the Mixed Membership Model (Section III-D). Section IV considers finite sample simulation studies of the proposed model and techniques. Section V illustrates the material in the paper with the real data example which demonstrates the advantage of keeping the edges' signs in the process of network construction. Proofs for all statements of the paper can be found in Appendix A.

II. CLUSTERING AND ESTIMATION TECHNIQUES

A. The DIMPLE-SGRDPG network: generation and assumptions

We generate a DIMPLE-SGRDPG network by first sampling group labels and subsequently obtaining SGRDPG networks in each group of layers using the standard protocols of [4].

Specifically, for each layer $l \in [L]$, we generate its group membership as

$$\begin{aligned} s(l) &\sim \text{Multinomial}(\vec{\pi}), \\ \vec{\pi} &= (\pi_1, \dots, \pi_M) \in [0, 1]^M, \quad \pi_1 + \dots + \pi_M = 1. \end{aligned} \quad (5)$$

In order to create the probability tensor \mathbf{P} , we generate M matrices $X^{(m)} \in [-1, 1]^{n \times K_m}$ with i.i.d. rows:

$$\begin{aligned} X^{(m)}(i, :) &\sim \text{i.i.d. } f_m, \quad \mathbb{E}(X^{(m)}(i, :)) = \mu^{(m)}, \\ \text{Cov}(X^{(m)}(i, :)) &= \Sigma^{(m)}, \quad m \in [M], \quad i \in [n], \end{aligned} \quad (6)$$

where f_m is a probability distribution on a subset of $[-1, 1]^{K_m}$. Subsequently, we consider a collection of symmetric matrices $B^{(l)} \in \mathbb{R}^{K_m \times K_m}$, $m = s(l)$, $l \in [L]$, and form the layer probability matrices $P^{(l)}$ as

$$P^{(l)} = X^{(m)} B^{(l)} (X^{(m)})^T. \quad (7)$$

It is easy to see that (7) is equivalent to the model (3). Indeed, if $X^{(m)} = U_X^{(m)} D_X^{(m)} O_X^{(m)}$ is the SVD of $X^{(m)}$, then (7) can be rewritten as (3) with

$$\begin{aligned} Q^{(l)} &= D_X^{(m)} O_X^{(m)} B^{(l)} (O_X^{(m)})^T D_X^{(m)}, \\ U^{(m)} &= U_X^{(m)}, \quad m = s(l), \quad l \in [L]. \end{aligned} \quad (8)$$

Note that we do not assume the elements of matrices $P^{(l)}$ to be non-negative: we merely require that entries of $P^{(l)}$ lie between -1 and 1. It is relatively easy to satisfy this assumption. In particular, if f_m is a distribution on the K_m -dimensional unit ball $\mathcal{B}(K_m)$ and all singular values of $B^{(l)}$ lie in $[-1, 1]$, then $P^{(l)}(i, j) \in [-1, 1]$, $i, j \in [n]$. Since $X^{(m)}$ and $B^{(l)}$ are defined up to a scaling constant, in what follows, we naturally assume that $X^{(m)}(i, :) \in \mathcal{B}(K_m)$, and model sparsity via matrices $B^{(l)}$, $l \in [L]$. We impose the following assumptions:

A1. Vector $\vec{\pi} = (\pi_1, \dots, \pi_M)$ is such that $\underline{c}_\pi M^{-1} \leq \pi_m \leq \bar{c}_\pi M^{-1}$, $m \in [M]$.

A2. Distributions f_m , $m \in [M]$, are supported on the K_m -dimensional unit balls $\mathcal{B}(K_m)$. Here, $K = \max_m K_m$ and $K \leq C_K \min_m K_m$ for some constant C_K .

A3. Covariance matrices $\Sigma^{(m)}$, $m \in [M]$, satisfy

$$0 < \underline{c} \leq \lambda_{\min}(\Sigma^{(m)}) \leq \lambda_{\max}(\Sigma^{(m)}) \leq \bar{c} < \infty. \quad (9)$$

A4. The number of layers L grows at most polynomially with respect to n . Specifically, for some constant τ_0

$$L \leq n^{\tau_0}, \quad 0 < \tau_0 < \infty. \quad (10)$$

A5. For some positive constants \underline{C}_B and \bar{C}_B , $0 < \underline{C}_B \leq \bar{C}_B < \infty$, one has

$$\begin{aligned} B^{(l)} &= \rho_n B_0^{(l)} \quad \text{with} \\ 0 < \underline{C}_B &\leq \sigma_{\min}(B_0^{(l)}) \leq \sigma_{\max}(B_0^{(l)}) \leq \bar{C}_B < \infty \end{aligned} \quad (11)$$

Note that Assumption **A1** as well as conditions on K_m are always satisfied if M is a constant independent of L and n . The constants in Assumptions **A3** and **A5** can be modified to depend on K_m . However, this will make the notations too cumbersome. For this reason, we impose uniform bounds in Assumptions **A3** and **A5**. Again, if M and K_m are constants independent of L and n , those constraints are easily justifiable. Assumption **A4** is hardly restrictive and is relatively common. Indeed, [25] assume that $L \leq n$, so, in their paper, (10) holds with $\tau_0 = 1$. We allow any polynomial growth of L with respect to n .

There are many ways of generating rows $X^{(m)}(i, :) \in \mathcal{B}(K_m)$ of matrices $X^{(m)}$, $i \in [n]$, $m \in [M]$, satisfying conditions (6) and (9). Below are some examples, where we suppress the index i .

- 1) f_m is a truncated normal distribution: $\xi \sim f_m$ is obtained as $\xi = \eta / \|\eta\|$ where $\eta \sim \mathcal{N}(\mu, \Sigma)$, the normal distribution with the mean μ and covariance Σ .

- 2) f_m is a truncated T -distribution with ν degrees of freedom: $\xi \sim f_m$ is obtained as $\xi = \eta / \|\eta\|$ where $\eta \sim T(\nu)$, the T -distribution with ν degrees of freedom.
- 3) Generate a vector $\eta \in [0, 1]^{K+1}$ as $\eta \sim \text{Dirichlet}(\vec{\alpha})$, where $\vec{\alpha} = (\alpha_1, \dots, \alpha_{K+1})$, $\alpha_k > 0$, $k \in [K+1]$. Set ξ to be equal to the first K components of η .
- 4) Generate a vector $\eta \in [0, 1]^{K+1}$ as $\eta \sim \text{Multinomial}(\vec{\varpi})$, where $\vec{\varpi} = (\varpi_1, \dots, \varpi_{K+1})$, $\varpi_k > 0$, $\varpi_1 + \dots + \varpi_{K+1} = 1$. Set ξ to be equal to the first K components of η .

Note that Examples 3 and 4 bring to mind, respectively, the Mixed Membership Model (MMM) and the Stochastic Block Model (SBM), where the last column of the community assignment matrix $X^{(m)}$ is missing. Indeed, in the case of the SBM or the MMM, rows of matrix $X^{(m)}$ sum to one, which means that covariance matrix of the rows of $X^{(m)}$ is singular and does not satisfy Assumption **A3**. However, as we see later in Section III-D, our methodology can handle the SBM or the MMM equipped networks, although Assumption **A3** does not hold in those cases.

B. Disentangling the DIMPLE-SGRDPG network: the between-layer clustering

Although matrices $X^{(m)}$ and, hence, $U_X^{(m)}$ are different for different values of m , they are too similar for ensuring a reliable separation of layers of the network, due to the common mean $\mu^{(m)}$ of rows of $X^{(m)}$, which implies that $\mathbb{E}(X^{(m)}) = 1_n \mu^{(m)}$, $m \in [M]$. For this reason, we “de-bias” the layers by removing this common mean and replacing $X^{(m)}$ with $\tilde{X}^{(m)} = X^{(m)} - 1_n \bar{X}^{(m)}$, where $\bar{X}^{(m)}$ is the sample mean of the rows of $X^{(m)}$. By introducing a projection operator $\Pi = n^{-1} 1_n 1_n^T$, we can rewrite $\tilde{X}^{(m)}$ as

$$\tilde{X}^{(m)} = X^{(m)} - \Pi X^{(m)} = \Pi^\perp X^{(m)}, \quad \Pi := n^{-1} 1_n 1_n^T. \quad (12)$$

It is easy to see that for $m \in [M]$, $l \in [L]$

$$\tilde{P}^{(l)} = \Pi^\perp P^{(l)} \Pi^\perp = \tilde{X}^{(m)} B^{(l)} (\tilde{X}^{(m)})^T, \quad s(l) = m. \quad (13)$$

Consider the SVDs of $\tilde{X}^{(m)}$ and $\tilde{P}^{(l)}$:

$$\tilde{X}^{(m)} = \tilde{U}^{(m)} \tilde{D}^{(m)} (\tilde{O}^{(m)})^T, \quad \tilde{P}^{(l)} = \tilde{U}_P^{(l)} D_P^{(l)} (\tilde{U}_P^{(l)})^T, \quad (14)$$

where $\tilde{O}^{(m)} \in \mathcal{O}_{K_m}$. Recall that $\tilde{P}^{(l)} = \tilde{U}^{(m)} \tilde{B}^{(l)} \tilde{U}^{(m)}$, where $\tilde{B}^{(l)} = \tilde{D}^{(m)} (\tilde{O}^{(m)})^T B^{(l)} \tilde{O}^{(m)} \tilde{D}^{(m)}$. Hence, one can rewrite the SVD of $\tilde{P}^{(l)}$ using the SVD $\tilde{B}^{(l)} = \tilde{U}_B^{(l)} \tilde{D}_B^{(l)} (\tilde{U}_B^{(l)})^T$ of $\tilde{B}^{(l)}$:

$$\tilde{P}^{(l)} = \tilde{U}^{(m)} \tilde{U}_B^{(l)} \tilde{D}_B^{(l)} (\tilde{U}^{(m)} \tilde{U}_B^{(l)})^T, \quad (15)$$

where $\tilde{U}_B^{(l)} \in \mathcal{O}_{K_m}$. Hence, it follows from (14) and (15) that $D_P^{(l)} = \tilde{D}_B^{(l)}$ and

$$\tilde{U}^{(m)} (\tilde{U}^{(m)})^T = \tilde{U}_P^{(l)} (\tilde{U}_P^{(l)})^T, \quad s(l) = m, \quad (16)$$

so that, the values of $\tilde{U}_P^{(l)} (\tilde{U}_P^{(l)})^T$ are unique for each group of layers $m \in [M]$.

This seems to be a trivial consequence of the observation, made in [37], that the values of $U_P^{(l)} (U_P^{(l)})^T$, where $U_P^{(l)}$ are the matrices of $K^{(m)}$ singular vectors of $P^{(l)}$, $l = s(m)$, are unique for each group of layers $m \in [M]$. However, we are

going to use this fact in a completely different way from [37]. Specifically, we show below that the scalar products of vectors $\text{vec}(\tilde{U}_P^{(l)}(\tilde{U}_P^{(l)})^T)$ are large if they belong to the same group of layers and are small otherwise. This actually means that vectors $\text{vec}(\tilde{U}_P^{(l)}(\tilde{U}_P^{(l)})^T)$ for different groups of layers form almost orthogonal subspaces. The latter however is not true for subspaces formed by vectors $\text{vec}(U_P^{(l)}(U_P^{(l)})^T)$ since all matrices $U_P^{(l)}$ include the vector $n^{-1/2} \mathbf{1}_n$ as a column (up to a rotation).

Therefore, in order to carry out between-layer clustering, for $l, l_1, l_2 \in [L]$, we denote

$$\theta^{(l)} = \text{vec}(\tilde{U}_P^{(l)}(\tilde{U}_P^{(l)})^T), \quad \Theta(l_1, l_2) = \langle \theta^{(l_1)}, \theta^{(l_2)} \rangle. \quad (17)$$

Furthermore, we calculate the sample-based versions of $\theta^{(l)}$ and exploit the fact the values of $\Theta(l_1, l_2)$ are small when $s(l_1) \neq s(l_2)$ and the same is true for their sample-based versions under the assumptions in Section II-A. The following statement confirms that $\theta^{(l)}$ are dissimilar enough to allow one to separate the network layers into groups.

Lemma 1. *Let Assumptions A1–A4 hold. If n is large enough, then, for any fixed constant τ , with probability at least $1 - CMn^{-\tau}$, one has*

$$\Theta(l_1, l_2) = K_m, \quad \text{if } s(l_1) = s(l_2) = m, \quad (18)$$

$$\max_{l_1, l_2} |\Theta(l_1, l_2)| \leq CKn^{-1} \log n, \quad \text{if } s(l_1) \neq s(l_2), \quad (19)$$

where constants C depend only on τ and the constants in Assumptions A1–A4.

The formal proof of Lemma 1 is given in the Appendix. Below, we give a brief explanation why it is true. If $s(l_1) = s(l_2) = m$, then $\Theta(l_1, l_2) = \|\theta^{(m)}\|^2 = \|\text{vec}(\tilde{U}^{(m)}(\tilde{U}^{(m)})^T)\|^2$, and it is easy to show that the first relation in (18) holds. In order to justify (19), consider the sample covariance matrices $\hat{\Sigma}^{(m)}$ with $\mathbb{E}(\hat{\Sigma}^{(m)}) = \Sigma^{(m)}$. If n is large enough, matrices $\hat{\Sigma}^{(m)}$ are both non-singular, and it follows from (14) that

$$\hat{\Sigma}^{(m)} = \frac{(\tilde{X}^{(m)})^T \tilde{X}^{(m)}}{n-1} = \frac{\tilde{O}^{(m)} (\tilde{D}^{(m)})^2 (\tilde{O}^{(m)})^T}{n-1}. \quad (20)$$

Denoting $(\hat{\Sigma}^{(m)})^{1/2} = (n-1)^{-1/2} \tilde{D}^{(m)} (\tilde{O}^{(m)})^T$ and $(\hat{\Sigma}^{(m)})^{-1/2} = (n-1)^{1/2} \tilde{O}^{(m)} (\tilde{D}^{(m)})^{-1}$, derive that

$$\tilde{U}^{(m)} = (n-1)^{-1/2} \tilde{X}^{(m)} (\hat{\Sigma}^{(m)})^{-1/2}. \quad (21)$$

It turns out that matrices $\tilde{X}^{(m)}$, $m \in [M]$, are dissimilar enough to allow separation of layers. In particular, the proof of (19) is based on the fact that, if n is large enough, the singular values of the true and the sample covariance matrices are close to each other and that, with high probability

$$\begin{aligned} \max_{l_1 \neq l_2} |\Theta(l_1, l_2)| &= O \left(n^{-2} \left\| \left(\tilde{X}^{(m_1)} \right)^T \tilde{X}^{(m_2)} \right\|_F^2 \right) \\ &= O(n^{-1} \log n). \end{aligned}$$

Note that, since the values of $\Theta(l_1, l_2)$ in (18) and (19) do not depend on matrices $B^{(l)}$, they are not affected by sparsity factor ρ_n , so their separation relies on the number n of nodes being large enough. Nevertheless, the accuracy of their sample counterparts depends on the sparsity factor ρ_n .

Algorithm 1: The between-layer clustering

Input: Adjacency tensor $\mathbf{A} \in \{0, 1, -1\}^{n \times n \times L}$; number of groups of layers M ; ambient dimension $K^{(l)}$ of each layer $l \in [L]$; parameter ϵ

Output: Estimated clustering function $\hat{s} : [L] \rightarrow [M]$ for groups of layers

Steps:

1: Find matrices $\hat{U}_A^{(l)} = \text{SVD}_{K^{(l)}}(\tilde{A}^{(l)})$ of $K^{(l)}$ left leading singular vectors of matrices

$$\tilde{A}^{(l)} = \Pi^\perp A^{(l)} \Pi^\perp, \quad l \in [L]$$

2: Form vectors $\hat{\theta}^{(l)} = \text{vec}(\hat{U}_A^{(l)}(\hat{U}_A^{(l)})^T)$, $l \in [L]$

3: Form matrix $\hat{\Theta}$ with elements

$$\hat{\Theta}(l_1, l_2) = \langle \hat{\theta}^{(l_1)}, \hat{\theta}^{(l_2)} \rangle, \quad l_1, l_2 \in [L]$$

4: Obtain matrix $\hat{V} = \text{SVD}_M(\hat{\Theta}) \in \mathcal{O}_{L,M}$ of M leading singular vectors of matrix $\hat{\Theta}$

5: Cluster L rows of \hat{V} into M clusters using $(1 + \epsilon)$ -approximate K -means clustering. Obtain estimated clustering function \hat{s}

C. The between-layer clustering algorithm

It is easy to see that Lemma 1 offers a path for the between-layer clustering. Consider proxies $\tilde{A}^{(l)} = \Pi^\perp A^{(l)} \Pi^\perp$ for $\tilde{P}^{(l)}$ in (13) and their full SVDs $\tilde{A}^{(l)} = \tilde{U}_A^{(l)} \tilde{D}_A^{(l)} (\tilde{U}_A^{(l)})^T$, $l \in [L]$. Note that $\text{rank}(\tilde{P}^{(l)}) = K_m$ where $m = s(l)$, so columns of $\tilde{U}_A^{(l)}$, beyond the first K_m ones, estimate pure noise. Since we do not know the grouping of the layers in advance, we instead have to deal with $K^{(l)} = \text{rank}(\tilde{P}^{(l)})$, where, of course, $K^{(l)} = K_m$ if $s(l) = m$. Specifically, we form matrices

$$\hat{U}_A^{(l)} = \text{SVD}_{K^{(l)}}(\tilde{A}^{(l)}), \quad \tilde{A}^{(l)} = \Pi^\perp A^{(l)} \Pi^\perp, \quad (22)$$

and, subsequently, construct vectors $\hat{\theta}^{(l)}$ and a matrix $\hat{\Theta}$ with components $\hat{\Theta}(l_1, l_2)$, $l, l_1, l_2 \in [L]$

$$\hat{\theta}^{(l)} = \text{vec}(\hat{U}_A^{(l)}(\hat{U}_A^{(l)})^T), \quad \hat{\Theta}(l_1, l_2) = \langle \hat{\theta}^{(l_1)}, \hat{\theta}^{(l_2)} \rangle. \quad (23)$$

Note that, since the values of K_m are not truly known before the between-layer clustering has been carried out, one can just replace K_m in the definition of T by $K^{(l)}$. The procedure above is summarized by Algorithm 1.

Remark 2. Recovering common left singular vectors. Note that in the model above, one can recover the common singular subspace U of all matrices $P^{(l)}$, $l \in [L]$, with high precision. This can be achieved, for example, by concatenating matrices $A^{(l)}$ into $A = [A^{(1)} | \dots | A^{(L)}]$ and estimating U by the set of the left singular vectors \tilde{U} of A . Alternatively, U can be estimated by the set of the left singular vectors of the unbiased sum of squares $(A^{(l)})^2$. It is known (see, e.g., [31]) that matrix U can be recovered with high precision if $\rho_n n L > C(\log n)^\nu$ for C and ν large enough. The latter however does not translate into easy clustering of layers.

To illustrate this issue, consider the case when $M = 2$, $K_1 = K_2 = K$ and $U^{(1)}$ and $U^{(2)}$ are the matrices of singular vectors in the two groups of layers. If $\tilde{U} = [U^{(1)} | U^{(2)}] \in R^{n \times 2K}$ has the SVD $\tilde{U} = U \Lambda_U O_U^T$ with $U \in \mathcal{O}_{n, 2K}$ and $O_U \in \mathcal{O}_{2K}$, then $P = U \tilde{P}$, where $\tilde{P} =$

$\Lambda_U O_U^T [\tilde{Q}^{(1)} \tilde{U}^T | \dots | \tilde{Q}^{(L)} \tilde{U}^T]$ and $\tilde{Q}^{(l)}$ are $(2K \times 2K)$ block-diagonal matrices with $\tilde{Q}_{1,1}^{(l)} \in \mathbb{R}^{K \times K}$ and $\tilde{Q}_{2,2}^{(l)} \in \mathbb{R}^{K \times K}$ on the diagonal. Here, $\tilde{Q}_{1,1}^{(l)} = Q^{(l)}$, $\tilde{Q}_{2,2}^{(l)} = 0$ if $s(l) = 1$, and $\tilde{Q}_{1,1}^{(l)} = 0$, $\tilde{Q}_{2,2}^{(l)} = Q^{(l)}$ if $s(l) = 2$. Now, suppose that matrix U is known (but, of course, we do not know $U^{(1)}$ and $U^{(2)}$). Then, our original goal would be replaced by the task of partitioning $(2K \times 2K)$ matrices $\Lambda_U O_U^T \tilde{Q}^{(l)} O_U \Lambda_U$ into two clusters. Since matrices $Q^{(l)}$ are arbitrary, this is not an easy undertaking. Indeed, matrix U acts in this setting as a nuisance parameter. It can easily be estimated but does not help much in clustering of layers into groups.

Remark 3. Unknown number of layers and ambient dimensions. While Algorithm 1 requires knowledge of M and ambient dimensions $K^{(l)}$ of each layer network, they may not be known in the case of real data. The assumption that these parameters are known is overwhelmingly common in methodological works, since the problem of finding the number of clusters is a very distinct problem from the process of actually solving the clustering problem with a known number of clusters. Since in the setting of this paper, the number of groups of layers and the ambient dimensions of those groups of layers coincide with the ranks of the respective matrices (specifically, Θ and $U^{(m)}$), there are many possible ways of accomplishing this task. In this paper, we estimate those quantities using the ScreeNOT technique of [15].

We further comment on using $K^{(l)}$ instead of K_m in Algorithm 1. While one can possibly assume that the values of K_m , $m \in [M]$, are known, this knowledge is hard to exploit since group labels are interchangeable and, therefore, in the case of non-identical subspace dimensions, it is hard to choose, which of the values corresponds to which of the groups. This is actually the reason why [17] and [25], who imposed this assumption, used it only in theory, while their simulations and real data examples are all restricted to the case of equal number of communities in all layers $K_m = K$, $m \in [M]$. On the contrary, knowledge of $K^{(l)}$ allows one to deal with different ambient dimensions in the groups of layers in simulations and real data examples. After the layers are partitioned into groups, due to $K^{(l)} = K_m$ when $m = s(l)$, the values of K_m should be re-fitted.

D. Fitting invariant subspaces in groups of layers

If we knew the true clustering matrix $S \in \mathcal{C}_{L,M}$ and the true probability tensor $\mathbf{P} \in \mathbb{R}^{n \times n \times L}$ with layers $P^{(l)}$ given by (3), then we could average layers with identical subspace structures. Precision of estimating matrices $U^{(m)}$, however, depends on whether the eigenvalues of $Q^{(l)}$ with $s(l) = m$ in (3) add up. Since the latter is not guaranteed, one can alternatively add the squares $G^{(l)} = (P^{(l)})^2$, obtaining matrices $H^{(m)}$, $m \in [M]$:

$$H^{(m)} = \sum_{s(l)=m} (P^{(l)})^2 = U^{(m)} \left[\sum_{s(l)=m} (Q^{(l)})^2 \right] (U^{(m)})^T. \quad (24)$$

In this case, the eigenvalues of $(Q^{(l)})^2$ are all positive which ensures successful recovery of matrices $U^{(m)}$. Note that,

Algorithm 2: Estimating invariant subspaces

Input: Adjacency matrices $\mathbf{A}^{(l)} \in \{0, 1, -1\}$, $l \in [L]$; number of groups of layers M ; ambient dimensions K_m of a group of layers $m \in [M]$; estimated layer clustering matrix $\hat{S} \in \mathcal{C}_{L,M}$

Output: Estimated invariant subspaces $\hat{U}^{(m)}$, $m \in [M]$

Steps:

1: Construct matrices $\hat{G}^{(l)}$, $l \in [L]$, and $\hat{H}^{(m)}$, $m \in [M]$ using (26)

2: For each $m \in [M]$, find $\hat{U}^{(m)}$ using formula (27)

however, $(A^{(l)})^2$ is not an unbiased estimator of $(P^{(l)})^2$. Indeed, while $\mathbb{E}[(A^{(l)})^2(i, j)] = [(P^{(l)})^2(i, j)]$ for $i \neq j$, for the diagonal elements, one has

$$\mathbb{E}[(A^{(l)})^2(i, i)] = (P^{(l)})^2(i, i) + \sum_j [(P^{(l)}(i, j) - (P^{(l)})^2(i, j))].$$

Therefore, we de-bias the squares $(A^{(l)})^2$ by subtracting the diagonal matrices $\hat{D}^{(l)}$ with elements

$$\hat{D}^{(l)}(i, i) = \sum_{j=1}^n |A^{(l)}(i, j)|, \quad \hat{D}^{(l)}(i, j) = 0 \quad \text{if } i \neq j, \quad (25)$$

and estimate $G^{(l)} = (P^{(l)})^2$, $l \in [L]$, and $\hat{H}^{(m)}$, $m \in [M]$, by, respectively,

$$\hat{G}^{(l)} = (A^{(l)})^2 - \hat{D}^{(l)}, \quad \hat{H}^{(m)} = \sum_{s(l)=m} \hat{G}^{(l)}. \quad (26)$$

After that, estimate $U^{(m)}$ by the matrix of K_m leading singular vectors of $\hat{H}^{(m)}$:

$$\hat{U}^{(m)} = \text{SVD}_{K_m}(\hat{H}^{(m)}), \quad m \in [M]. \quad (27)$$

The procedure is summarized in Algorithm 2.

Remark 4. Alternative techniques for estimating ambient subspaces. Note that one can estimate bases $\hat{U}^{(m)}$ of the ambient subspaces using alternative techniques. For example, in the COSIE model, which corresponds to $M = 1$ in our setting, [4] used spectral embedding. The methodology is based on constructing matrices $\hat{U}^{(l)} = \text{SVD}_K(A^{(l)})$, $l \in [L]$, and subsequently placing them, side by side, forming a new matrix $\tilde{U} = [U^{(1)} | \dots | U^{(L)}] \in \mathbb{R}^{n \times KL}$. The estimator \tilde{U} of U is then obtained as $\tilde{U} = \text{SVD}_K(\tilde{U})$. Another way of estimating $\hat{U}^{(m)}$ is to follow the technique of, e.g., [26] where, in the case of $M = 1$, adjacency matrices $A^{(l)}$ are placed side by side to form one matrix \tilde{A} , and the common matrix U of the left singular vectors of $P^{(l)}$, $l \in [L]$, is then estimated by the matrix of the left singular vectors \tilde{U} of \tilde{A} . We shall compare the latter technique with our Algorithm 2 in Section IV.

III. THEORETICAL ANALYSIS

A. Error measures

In this section, we study the between-layer clustering error rates of Algorithm 1 and the error of estimation of invariant subspaces of Algorithm 2. Since clustering is unique only

up to a permutation of cluster labels, denote the set of K -dimensional permutation functions of $[K]$ by $\aleph(K)$, and the set of $(K \times K)$ permutation matrices by $\mathfrak{F}(K)$. The misclassification error rate of the between-layer clustering is then given by

$$R_{BL} = (2L)^{-1} \min_{\mathcal{P} \in \mathfrak{F}(M)} \|\hat{S} - S\mathcal{P}\|_F^2. \quad (28)$$

In order to assess the accuracy of estimating matrices $U^{(m)}$ by $\hat{U}^{(m)}$, $m \in [M]$, we use the $\sin \Theta$ distances that allow to take into account that matrices $\hat{U}^{(m)}$ are unique only up to an arbitrary rotation. The $\sin \Theta$ distances between two subspaces with orthonormal bases $U \in \mathcal{O}_{n,K}$ and $\hat{U} \in \mathcal{O}_{n,K}$, respectively, are defined as follows ([8]). Suppose the singular values of $U^T \hat{U}$ are $\sigma_1 \geq \sigma_2 \geq \dots \geq \sigma_K > 0$. The quantitative measures of the distance between the column spaces of U and \hat{U} are then

$$\begin{aligned} \|\sin \Theta(U, \hat{U})\| &= \left(1 - \sigma_K^2(U^T \hat{U})\right)^{1/2}, \\ \|\sin \Theta(U, \hat{U})\|_F &= \left(K - \|U^T \hat{U}\|_F^2\right)^{1/2}. \end{aligned}$$

We also define

$$D(U, \hat{U}; 2, \infty) = \min_{W \in \mathcal{O}_K} \|\hat{U}W - U\|_{2,\infty} \quad (29)$$

and observe that $D(U, \hat{U}; 2, \infty) \leq \sqrt{2} \|\sin \Theta(U, \hat{U})\|$ (see, e.g., [8]). Since the numbering of groups of layers is defined up to a permutation, we need to minimize those errors over the permutation of labels. In particular, we measure the precision of subspace estimation by

$$R_{U,2,\infty} = \min_{\aleph(M)} \max_{m \in [M]} D\left(U^{(m)}, \hat{U}^{(\aleph(m))}; 2, \infty\right), \quad (30)$$

$$R_{U,ave}^2 = \frac{1}{M} \min_{\aleph(M)} \sum_{m=1}^M \left\| \sin \Theta\left(U^{(m)}, \hat{U}^{(\aleph(m))}\right) \right\|_F^2, \quad (31)$$

$$R_{U,\max} = \min_{\aleph(M)} \max_{m \in [M]} \left\| \sin \Theta\left(U^{(m)}, \hat{U}^{(\aleph(m))}\right) \right\|. \quad (32)$$

B. The accuracy of the between-layer clustering

Successful between-layer clustering relies on the fact that the elements of the true Gramm matrix $\Theta(l_1, l_2)$ in (18) and (19) are large, when $s(l_1) = s(l_2)$, and are small otherwise. In practice, those values are unavailable, and one has to use their sample substitutes in Algorithm 1. It is obvious that the between-layer clustering errors depend on whether matrix $\hat{\Theta}$ in (23) inherits the properties of Θ . It turns out that the latter is true if n is large enough and the layers are not too sparse. Specifically, the following statement holds.

Lemma 2. *Let Assumptions A1–A5 hold and matrix $\hat{\Theta}$ be defined in (23). If the layers of the network are moderately sparse, so that*

$$n \rho_n \geq C_\rho \log n, \quad (33)$$

then, if n is large enough, for any fixed constant τ , uniformly, with probability at least $1 - Cn^{-(\tau-\tau_0)}$, one has

$$\hat{\Theta}(l_1, l_2) \geq K_m \left[1 - C(n\rho_n)^{-\frac{1}{2}}\right] \text{ if } s(l_1) = s(l_2) = m, \quad (34)$$

$$|\hat{\Theta}(l_1, l_2)| \leq C K (n\rho_n)^{-1/2} \text{ if } s(l_1) \neq s(l_2), \quad (35)$$

where constants C depend only on τ and the constants in Assumptions A1–A5.

While we state that n has to be large enough in order Lemma 2 holds, we provide an exact inequality for the lower bound on n in formula (91) of Section A-D, which ensures that Lemma 2 and subsequent statements are valid.

Note that condition (33) is very common in the random networks models. If a random network follows the SBM, then condition (33) is necessary and sufficient for adequate community recovery ([19]). Since in our multiplex network the layers are grouped on the basis of subspace similarities, it is only natural that assumption (33) appears in our theory. Indeed, this assumption is present in a number of papers that consider simpler multilayer GRDPG models, such as COSIE in [4] and [46], or the Multilayer Degree-Corrected Stochastic Blockmodels in [1].

Theorem 1. *Let layer assignment function \hat{s} be obtained by Algorithm 1 with $K^{(l)} = K_m$, $m = s(l)$. Let Assumptions A1–A5 and condition (33) hold, and*

$$\lim_{n \rightarrow \infty} K M^2 \log n (n \rho_n)^{-1} = 0. \quad (36)$$

If n is large enough, so that condition (91) is valid, then, for any fixed constant τ and C_τ that depends only on τ and constants in Assumptions A1–A5, one has

$$\mathbb{P}(R_{BL} = 0) = \mathbb{P}(\hat{s} = s) \geq 1 - C n^{-\tau}. \quad (37)$$

Hence, Algorithm 1 delivers strongly consistent clustering with high probability.

Remark 5. Comparison with results of Pensky and Wang (2024). Observe that the between-layer clustering error rates are much smaller than in [37] where it is shown, that under similar assumptions, with high probability, $R_{BL} = O(\sqrt{\log n (n\rho_n)^{-1/2}})$ as $n \rightarrow \infty$. The rates in Theorem 1 are similar to the ones, obtained in [35], for a much simpler network with the SBM-equipped sign-free layers. In addition, [35] used a methodology that does not work for a network with the GRDPG-equipped layers.

C. The subspace fitting errors in the groups of layers

In this section, we provide upper bounds for the divergence between matrices $U^{(m)}$ and their estimators $\hat{U}^{(m)}$, $m \in [M]$, delivered by Algorithm 2. We measure their discrepancies by $R_{U,ave}$ and $R_{U,\max}$ defined in (31) and (32), as well as by $R_{U,2,\infty}$ defined in (30). The upper bounds for $R_{U,ave}$ and $R_{U,\max}$ are presented below in Theorem 2.

Theorem 2. *Let Assumptions of Theorem 1 hold. Let matrices $\hat{U}^{(m)}$, $m \in [M]$, be obtained using Algorithm 2 and*

$$L \geq 2(\underline{c}_\pi)^{-2} M^2 \log(n^{\tau+2\tau_0}). \quad (38)$$

Then, for any $\tau > 0$, and absolute constants C_τ that depend on τ and constants in Assumptions **A1**–**A5** only, with probability at least $1 - C n^{-(\tau-2(\tau_0+1))}$, one has

$$\begin{aligned} R_{U,\max} &\leq C_\tau \left(\frac{\sqrt{M \log n}}{\sqrt{\rho_n n L}} + \frac{1}{n} \right), \\ R_{U,\text{ave}} &\leq C_\tau \left(\frac{\sqrt{K M \log n}}{\sqrt{\rho_n n L}} + \frac{\sqrt{K}}{n} \right). \end{aligned} \quad (39)$$

While the proof of Theorem 2 follows the lines of the proofs in [37] and [35], construction of an upper bound for $R_{U,2,\infty}$ requires novel techniques.

Theorem 3. *Let Assumptions of Theorem 2 hold. Then, for any $\tau > 0$, and absolute constant C_τ that depends on τ and constants in Assumptions **A1**–**A5** only, with probability at least $1 - C n^{-(\tau-\tau_0-1)}$, one has*

$$R_{U,2,\infty} \leq C_\tau \frac{\sqrt{K}}{\sqrt{n}} \left[\frac{\sqrt{M \log n}}{\sqrt{\rho_n n L}} + \frac{1}{n} \right] \left(1 + \frac{\sqrt{M \log n}}{\rho_n \sqrt{n L K}} \right). \quad (40)$$

Corollary 1. *Let Assumptions of Theorem 2 hold with $M = 1$. Then, with probability at least $1 - C n^{-(\tau-\tau_0-1)}$, one has*

$$R_{U,2,\infty} \leq C_\tau \frac{\sqrt{K}}{\sqrt{n}} \left[\frac{\sqrt{\log n}}{\sqrt{\rho_n n L}} + \frac{1}{n} \right] \left(1 + \frac{\sqrt{\log n}}{\rho_n \sqrt{n L K}} \right). \quad (41)$$

Observe that the errors in (40) and (41) are products of three terms. The middle terms in the square parentheses are the upper bounds of the errors of subspace recovery in operational norm. The first factor, \sqrt{K}/n is the main improvement effect of using the $(2, \infty)$ rather than operational norm. The last multipliers are the correction terms, that are due to the fact that, in the expansion for the $(2, \infty)$ errors, the operational norm is multiplied by a factor that can be potentially larger than \sqrt{K}/n . The value of this term depends on sparsity ρ_n , the number of layers L and on n and K . It is easy to see that the term is bounded above if the network is not too sparse, or if L is large enough.

Note that, although we consider symmetric layer networks in this paper, we believe that, with minimal adjustments, the same methodology can be applied to directed networks with $P^{(l)} = U^{(m)} B^{(l)} V^{(m)}$, $m \in [M]$, $l \in [L]$. Setting $M = 1$ would then provide the $(2, \infty)$ error bound in the undirected COSIE model of [46].

Remark 6. Estimation of the loading matrices. While in our setting, matrices $Q^{(l)}$ in (1) are just nuisance parameters, one can imagine a scenario where those matrices may exhibit some behavior of interest and, hence, need to be estimated. Since under conditions of Theorem 1, clustering is perfect with high probability when n is large enough, the model reduces to the COSIE model for each group of clusters. Therefore, one can essentially repeat all results that were obtained for the COSIE model. Specifically, since one can estimate $U^{(m)}$, $m \in [M]$, with high precision, the errors of estimating $Q^{(l)}$ will be dominated by the portions originated from the differences between $A^{(l)}$ and $P^{(l)}$.

Remark 7. Comparison with competitive results. Observe also that the average subspace recovery errors in (39) are similar to the rates, obtained in [4] for the COSIE model. They are considerably lower than the errors in [37], where it is proved that, with high probability,

$$\begin{aligned} R_{U,\text{ave}} &\leq C_\tau \left\{ I(M > 1) \frac{\sqrt{K^5 M \log n}}{\sqrt{n \rho_n}} \left[1 + \frac{K \log n}{\sqrt{n \rho_n}} \right] \right. \\ &\quad \left. + \frac{\sqrt{K^5 M \log n}}{\sqrt{n L \rho_n}} + \frac{K^{5/2}}{n} \right\}. \end{aligned}$$

Moreover, due to similarities between the algorithms, they are similar to the errors in [31]: the seeming difference comes from the fact that [31] study sparser networks with $n \rho_n \leq C$ where C is a constant.

As it is expected, the error rate $R_{U,2,\infty}$ of subspace recovery in $(2, \infty)$ -norm is consistently smaller than the rate $R_{U,\max}$ in operational norm. Specifically, it follows from (39) and (40) that, under condition (33), one has, as $n \rightarrow \infty$

$$R_{U,2,\infty}/R_{U,\max} \propto \left[\sqrt{K/n} + \sqrt{\log n}/(\rho_n n \sqrt{L}) \right] \rightarrow 0$$

for any L . Note that the latter is not true for [46], who studied the COSIE model, corresponding to $M = 1$. Specifically, in our notations, under the assumption that $\|U\|_{2,\infty} \leq C K^{1/2} n^{-1/2}$, they derived that

$$\min_{W \in \mathcal{O}_K} \|\hat{U} W - U\|_F \leq C \sqrt{K} (L n \rho_n)^{-1/2}, \quad (42)$$

$$\begin{aligned} \min_{W \in \mathcal{O}_K} \|\hat{U} W - U\|_{2,\infty} &\leq C \left[(K \log n)^{1/2} (L n^2 \rho_n)^{-1/2} \right. \\ &\quad \left. + K^{1/2} n^{-1/2} \log n (n \rho_n)^{-1} \right]. \end{aligned} \quad (43)$$

Therefore, (42) and (43) imply that, in their case,

$$\frac{\min_{W \in \mathcal{O}_K} \|\hat{U} W - U\|_{2,\infty}}{\min_{W \in \mathcal{O}_K} \|\hat{U} W - U\|_F} \propto \frac{\sqrt{K}}{\sqrt{n}} + \frac{\sqrt{L \log n}}{\sqrt{n^2 \rho_n}}. \quad (44)$$

Observe that the second term tends to infinity if L grows polynomially faster than n and $n \rho_n \asymp (\log n)^{a+1}$ for some constant $a > 0$. Note also that the $R_{U,2,\infty}$ error of Algorithm 2 is **significantly smaller** than that of [46]. We do not know whether the latter is due to a shortcoming of their algorithm, or the deficiency of their proof.

D. The Stochastic Block Model and the Mixed Membership Model

Observe that in the case of the multiplex network where layers are equipped with the SBM or MMM, one has $X^{(m)} = Z^{(m)}$, where $Z^{(m)}$ are membership matrices, so that each row of matrix $Z^{(m)}$ sums to one. The latter leads to all covariance matrices $\Sigma^{(m)}$ being singular. Nevertheless, Algorithms 1 and 2 can still be successfully applied, albeit with very minor modifications.

Indeed, Algorithm 1 starts with replacing matrices $A^{(l)}$ with $\tilde{A}^{(l)} = \Pi^\perp A^{(l)} \Pi^\perp$, $l \in [L]$. In the case when Assumption **A3** holds, matrices $\tilde{A}^{(l)}$ are proxies for matrices $\tilde{P}^{(l)}$ of rank K_m where $m = s(l)$. If the layer graphs are generated by the SBM or the MMM, one has $\text{rank}(\tilde{P}^{(l)}) = K_m - 1$. This, however,

does not matter as long as one treats $K^{(l)}$ as the rank of $\tilde{P}^{(l)}$, $l \in [L]$, so that $K^{(l)} = K_m - 1$ for $s(l) = m$.

In order to see why this is true, consider the situation where, similarly to (6), one has $X^{(m)}(i, :) \sim \text{i.i.d. } f_m$, $i \in [n]$, and f_m , $m \in [M]$, are such that $X^{(m)}(i, :)1_{K_m} = 1$ but covariance matrices of the first $(K_m - 1)$ components of row vectors $X^{(m)}(i, :)$ are non-singular. In order to formalize the discussion above, we introduce matrices $\check{X}^{(m)} = X^{(m)}(:, 1 : K_m - 1)$ which consist of the first $K_m - 1$ columns of matrices $X^{(m)}$ and denote their covariance matrices by $\check{\Sigma}^{(m)} = \text{Cov}(\check{X}(i, :)) \in \mathbb{R}^{(K_m-1) \times (K_m-1)}$. We assume that f_m are such that

$$\begin{aligned} X^{(m)}1_{K_m} &= 1_n, \quad m \in [M], \\ 0 < \underline{c} \leq \lambda_{\min}(\check{\Sigma}^{(m)}) &\leq \lambda_{\max}(\check{\Sigma}^{(m)}) \leq \bar{c} < \infty. \end{aligned} \quad (45)$$

Note that the first condition in (45) holds for both the SBM and the MMM. The second condition in (45) can be guaranteed by a variety of assumptions. In this paper, as one of the options, we assume that, in the cases of the SBM and the MMM, f_m are, respectively, the Multinomial($\alpha^{(m)}$) or the Dirichlet($\alpha^{(m)}$) distributions, where vectors $\alpha^{(m)}$ are such that

$$\underline{c}_\alpha/K \leq \alpha_k^{(m)} \leq \bar{c}_\alpha/K, \quad m \in [M]. \quad (46)$$

Partition each matrix $B^{(l)}$, $s(l) = m$, into the three portions: matrix $\tilde{B}^{(l)} = B^{(l)}(1 : K_m - 1, 1 : K_m - 1)$, vector $\tilde{b}^{(l)} = B^{(l)}(1 : K_m - 1, K_m)$ and a scalar $B^{(l)}(K_m, K_m)$. Introduce $\check{b}^{(l)} = \tilde{b}^{(l)} - B^{(l)}(K_m, K_m)1_{K_m-1}$ and

$$\begin{aligned} \check{B}^{(l)} &= \tilde{B}^{(l)} - \tilde{b}^{(l)}(1_{K_m-1})^T - 1_{K_m-1}(\tilde{b}^{(l)})^T \\ &\quad + B^{(l)}(K_m, K_m)1_{K_m-1}(1_{K_m-1})^T. \end{aligned} \quad (47)$$

Observe that $\check{B}^{(l)} = J^{(m)}B^{(l)}(J^{(m)})^T$ where matrix $J^{(m)}$ is a horizontal concatenation of I_{K_m-1} , the $(K_m - 1)$ -dimensional identity matrix, and the vector -1_{K_m-1} . Rewrite $P^{(l)}$ as $P^{(l)} = \check{X}^{(m)}\check{B}^{(l)}(\check{X}^{(m)})^T + \check{X}^{(m)}\check{b}^{(l)}1_n^T + 1_n(\check{X}^{(m)}\check{b}^{(l)})^T + B^{(l)}(K_m, K_m)$. While $P^{(l)}$ cannot be expressed via $\check{X}^{(m)}$ and $\check{B}^{(l)}$, matrices $\tilde{P}^{(l)}$ in (13) can:

$$\begin{aligned} \tilde{P}^{(l)} &= \check{X}^{(m)}\check{B}^{(l)}(\check{X}^{(m)})^T, \\ \check{B}^{(l)} &= J^{(m)}B^{(l)}(J^{(m)})^T, \quad J^{(m)} = [I_{K_m-1} | -1_{K_m-1}]. \end{aligned} \quad (48)$$

Here, matrices $\check{X}^{(m)}$ are such that condition (45) holds and can replace Assumption A3. Moreover, since all singular values of $J^{(m)}$ lie between 1 and $\sqrt{K_m}$, matrices $\check{B}^{(l)}$ satisfy the assumption which is equivalent to the Assumption A5

$$\check{B}^{(l)} = \rho_n \check{B}_0^{(l)} \quad \text{with} \quad \sigma_{\min}(\check{B}_0^{(l)}) \geq \underline{C}_B > 0. \quad (49)$$

Therefore, one obtains an immediate corollary of Theorem 1.

Corollary 2. *Let distributions f_m and matrices $B^{(l)}$ satisfy Assumptions A1, A2, A4, A5 and (45). Let the layer assignment function \hat{s} be obtained by Algorithm 1 with $K^{(l)} = K_m - 1$, $m = s(l)$, where $\min_m K_m \geq 2$. Let (33) and (36) hold. Then, if n is large enough, for any fixed constant τ , (37) is valid, so that Algorithm 1 delivers strongly consistent layer clustering with high probability.*

Algorithm 3: The between-layer clustering of [37]

Input: Adjacency tensor $\mathbf{A} \in \{0, 1\}^{n \times n \times L}$; number of groups of layers M ; ambient dimension $K^{(l)}$ of each layer $l \in [L]$; parameter ϵ

Output: Estimated clustering function $\hat{s} : [L] \rightarrow [M]$ for groups of layers

Steps:

- 1: Find matrices $\hat{U}_A^{(l)} = \text{SVD}_{K^{(l)}}(A^{(l)})$ of $K^{(l)}$ left leading singular vectors of matrices $A^{(l)}$
 - 2: Form matrix $\tilde{\Theta} \in \mathbb{R}^{n^2 \times L}$ with columns $\tilde{\Theta}(:, l) = \text{vec}(\hat{U}_{A,l}(\hat{U}_{A,l})^T)$, $l \in [L]$
 - 3: Find matrix $\tilde{W} = \text{SVD}_M(\tilde{\Theta}^T) \in \mathcal{O}_{L,M}$ of M leading singular vectors of matrix $\tilde{\Theta}^T$
 - 4: Cluster L rows of \tilde{W} into M clusters using $(1 + \epsilon)$ -approximate K -means clustering. Obtain estimated clustering function \hat{s}
-

IV. SIMULATION STUDY

A. Simulations settings

A limited simulation study, described in this section, has a dual purpose. The first goal is to show that our techniques deliver accurate cluster assignments and ambient subspace estimators in a finite sample case. Since to the best of our knowledge, the only other paper that considers the multilayer GRDPG with groups of layers is [37], we carry out finite sample comparisons with the between-layer clustering in [37] (Algorithm 3). We do not exhibit the comparison of the ambient subspaces recovery for those cases since the construction of the unbiased tensor of squared averages in [37] needs to be modified due to the presence of signs, and Algorithm 2 carries out this modification.

Instead, we compare our within-layer clustering technique with the one used in [26] where adjacency matrices $A^{(l)}$ are placed side by side to form one matrix \tilde{A} , and the common matrix of the left singular vectors of $P^{(l)}$, $l \in [L]$, is then estimated by the matrix of the left singular vectors of \tilde{A} (see Remark 4). In order the comparison is fair, we use Algorithm 1 for the between-layer clustering for both their method and Algorithm 2.

The second goal is to demonstrate advantages of the model itself. Indeed, in many applications, when a network is constructed and edges are drawn, the associated edges' signs are removed, and the adjacency matrix has 0/1 entries only. In our simulations examples, we show that by just keeping the sign and allowing the entries of the adjacency matrix take 0/1/-1 values, one can significantly improve the accuracy of the analysis of the network.

In order to attain those objectives, we examine the SGRDPG multiplex networks with matrices $X^{(m)}$, $m \in [M]$, generated by the following four distributions described in Section II-A:

Case 1. f_m is a truncated normal distribution, so that $\xi \sim f_m$ is obtained as $\xi = \eta/\|\eta\|$, where η is a K -dimensional vector with components being i.i.d. normal with mean zero and variance σ^2 .

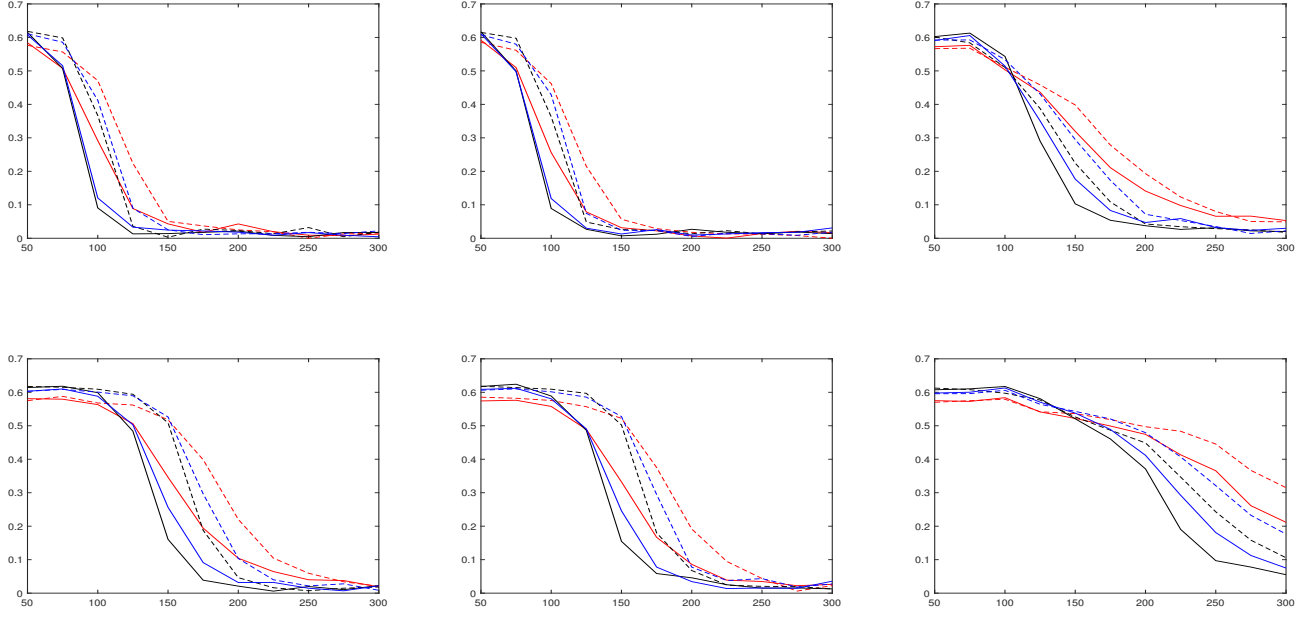


Fig. 1. The between-layer clustering errors R_{BL} in (28) of Algorithms 1 (solid lines) and Algorithms 3 (dash lines). Matrices $X^{(m)}$ are generated by the truncated normal distribution with $\sigma = 1$, $\mu = 0$ (left panels), the truncated T -distribution with $\nu = 2$ (middle panels) and the truncated Dirichlet distribution with $\alpha_k = \alpha = 0.1$, $k \in [K_m + 1]$ (right panels). In all cases, $M = 3$ and $K_m = K = 3$. The entries of $B^{(l)}$ are generated as uniform random numbers between $c = -0.05$ and $d = 0.05$ (top row) and $c = -0.03$ and $d = 0.03$ (bottom row). Errors are averaged over 100 simulation runs, $L = 50$ (red), $L = 100$ (blue), $L = 150$ (black).

Case 2. f_m is a truncated T -distribution with ν degrees of freedom: $\xi \sim f_m$ is obtained as $\xi = \eta/\|\eta\|$ where $\eta \sim T(\nu)$, the T -distribution with ν degrees of freedom.

Case 3. f_m is a reduced Dirichlet distribution, so that $\xi \sim f_m$ is obtained as the first K components of vector $\eta \in [0, 1]^{K+1}$, where $\eta \sim \text{Dirichlet}(\vec{\alpha})$ with $\vec{\alpha} = (\alpha_1, \dots, \alpha_{K+1})$, $\alpha_k > 0$, $k \in [K + 1]$.

Case 4. f_m is a the multinomial distribution, so that $\xi \sim f_m$ is obtained as $\eta \sim \text{Multinomial}(\vec{\varpi})$, where $\vec{\varpi} = (\varpi_1, \dots, \varpi_K)$, $0 \leq \varpi_k \leq 1$, $\varpi_1 + \dots + \varpi_K = 1$. Observe that in this case, distribution f_m does not satisfy Assumption A3 and leads to the Signed SBM studied in the Section III-D.

In order to obtain the DIMPLE-SGRDPG network, we fixed the number of groups of layers M and the ambient dimension of each group of layers K_m . We generate group membership of each layer $l \in [L]$, using the Multinomial distribution as described in (5) with $\pi_m = 1/M$. After that, we generate M matrices $X^{(m)} \in [-1, 1]^{K_m}$ with i.i.d. rows using (6), where f_m is one of the four distributions above. Next, we generate the above diagonal entries of symmetric matrices $B^{(l)}$, $l \in [L]$, in (7) as uniform random numbers between c and d . Then, connection probability matrices $P^{(l)}$, $l \in [L]$, are of the form (7). The common bases of the ambient subspaces $U^{(m)}$ in groups of layers are formed by the K left singular vectors of matrices $X^{(m)}$, and matrices $Q^{(l)}$ in (3) are of the forms (8). Subsequently, the layer adjacency matrices $A^{(l)}$ are generated according to (2). The code is available from the author's website at

<https://sciences.ucf.edu/math/mpensky/recent-publications/>

B. Between-layer clustering simulations comparisons with the technique of Pensky & Wang (2024)

In this section, we compare the between-layer clustering assignments using Algorithm 1 and Algorithm 3 of [37] in the cases of the truncated normal distribution, the truncated T -distribution and the truncated Dirichlet distribution with $M = 3$, $K_m = K = 3$ and two sparsity settings. Results are presented in Figure 1.

As Figure 1 demonstrates, even for such a sparse networks the between layer clustering errors are decreasing rapidly, as n grows, and are declining slowly as L increases. It is also easy to see that the between layer clustering errors of Algorithm 3 in [37] remain larger than the respective errors of Algorithm 1.

C. Comparison of the ambient subspace estimation techniques

In this section we compare the ambient subspace estimation precision of Algorithm 2 and the algorithm of [26] described in Remark 4. Here, we exhibit results for the examples considered in the previous section, that is, the cases of the normal distribution, the T -distribution and the Dirichlet distribution with $M = 3$, $K_m = K = 3$ and two sparsity settings. In all examples in this section, the between-layer clustering is carried out using Algorithm 1.

We measure the deviations between ambient subspaces in the two-to-infinity norm defined in (29). Specifically, instead of trying to find a matrix W that delivers the minimum in (29), we are using its Frobenius proxy W_U defined as follows. If $\hat{U}^T U = O_1 D_U O_2^T$ is the SVD of $\hat{U}^T U$, then $W_U = O_1 O_2^T$. Hence, for $m \in [M]$, we replace $D(U^{(m)}, \hat{U}^{(m)}; 2, \infty)$ with

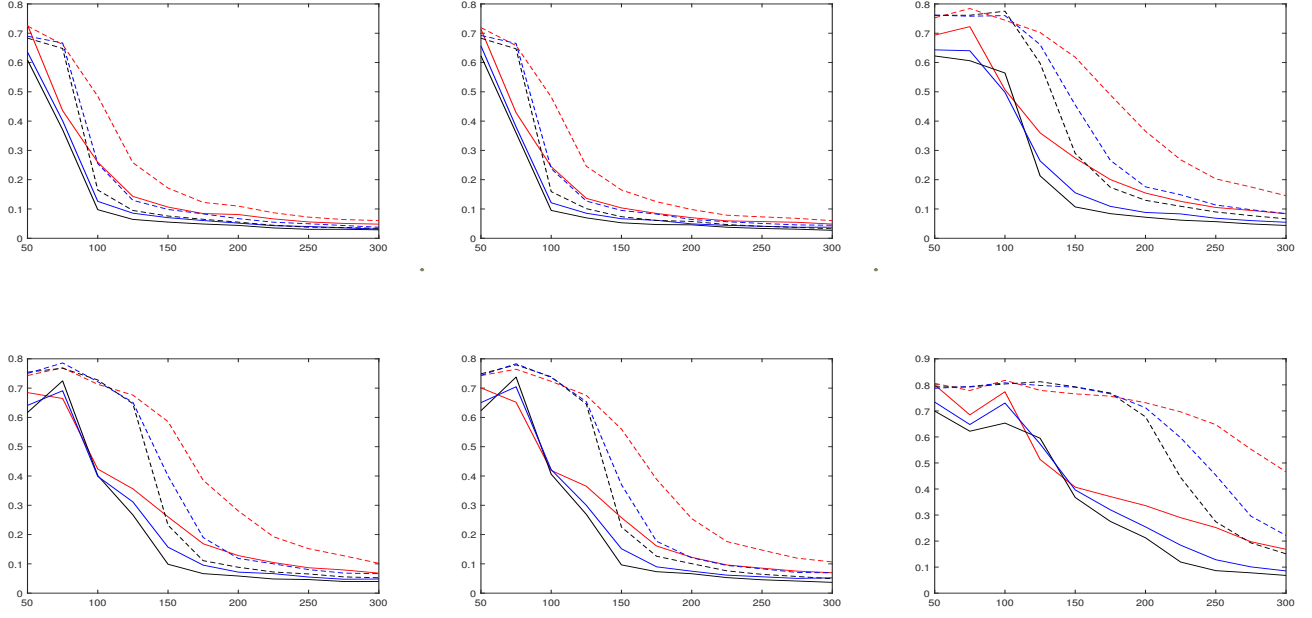


Fig. 2. The subspace estimation errors $R_{2,\infty,ave}$ in (50) of Algorithms 2 (solid lines) and of the Algorithm described in Remark 4 (dash lines). Matrices $X^{(m)}$ are generated by the truncated normal distribution with $\sigma = 1$, $\mu = 0$ (left panels), the truncated T -distribution with $\nu = 2$ (middle panels) and the truncated Dirichlet distribution with $\alpha_k = \alpha = 0.1$, $k \in [K_m + 1]$ (right panels). In all cases, $M = 3$ and $K_m = K = 3$. The entries of $B^{(l)}$ are generated as uniform random numbers between $c = -0.05$ and $d = 0.05$ (top row) and $c = -0.03$ and $d = 0.03$ (bottom row). Errors are averaged over 100 simulation runs, $L = 50$ (red), $L = 100$ (blue), $L = 150$ (black).

$\|\hat{U}^{(m)} W_U^{(m)} - U^{(m)}\|_{2,\infty}$, where $\hat{U}^{(m)}$ is the best match for $U^{(m)}$ over all permutations of $m \in [M]$. Subsequently, we evaluate the errors as the averages of those quantities:

$$R_{2,\infty,ave} = M^{-1} \sum_{m=1}^M \|\hat{U}^{(m)} W_U^{(m)} - U^{(m)}\|_{2,\infty}, \quad (50)$$

where $W_U^{(m)} = O_1^{(m)} (O_2^{(m)})^T$ and $(\hat{U}^{(m)})^T U^{(m)} = O_1^{(m)} D_U^{(m)} (O_2^{(m)})^T$ is the SVD of $(\hat{U}^{(m)})^T U^{(m)}$.

Results are presented in Figure 2. As it is evident from Figure 2, Algorithm 2 always delivers higher accuracy than the algorithm suggested in [26]. The differences between the performances between the algorithms become more acute when the networks are getting sparser. The superior accuracy of Algorithm 2 follows from de-biasing, as it is shown in [31].

D. Comparison with the networks where signs are removed

In order to study the effect of removing the signs of the entries of matrices $A^{(l)}$, for each simulation run, we carry out a parallel inference with matrices $P^{(l)}$ and $A^{(l)}$ replaced by $|P^{(l)}|$ and $|A^{(l)}|$, where $|Y|$ denotes the matrix which contains absolute values of the entries of matrix Y . We denote the tensors with absolute values, corresponding to \mathbf{P} and \mathbf{A} , by $|\mathbf{P}|$ and $|\mathbf{A}|$, respectively.

We consider two examples of the SGRDPG networks, one where the ambient subspaces of the layers of the network are generated using by Dirichlet distribution (Case 2), and another, where layers are equipped with the true SBM (Case 3). The reason for those choices is that, in both cases, it is easy to trace the impact of removing signs on the probability tensor.

Specifically, the latter will correspond to removing the signs in the matrices of block probabilities $B^{(l)}$, $l \in [L]$, in (7).

Same as before, in our simulations, we use Algorithm 1 for clustering layers $A^{(l)}$ and $|A^{(l)}|$, $l \in [L]$, into M groups, and determine the precision of the partition using the between-layer clustering error rate (28). In the case of the SBM, subsequently, we estimate the bases of the ambient subspaces in each of M groups of layers, using Algorithm 2, and cluster the rows by $(1+\epsilon)$ -approximate K -means clustering, obtaining community assignments for each group of layers. We measure the accuracy of the community assignment in groups of layers by the average within-layer clustering error given by

$$\begin{aligned} R_{WL} &= \frac{1}{M} \min_{\mathfrak{N}(M)} \sum_{m=1}^M R_{WL}(m) \\ &= \frac{1}{2Mn} \min_{\mathfrak{N}(M)} \sum_{m=1}^M \left[\min_{\mathcal{P}_m \in \mathfrak{F}(K_m)} \|\hat{\mathbf{Z}}^{(m)} - \mathbf{Z}^{(m)} \mathcal{P}_m\|_F^2 \right]. \end{aligned} \quad (51)$$

Simulations results are presented in Figure 3.

It is clear from all three of the figures that the removal of the signs of the edges is extremely detrimental to network analysis. The effects are much more dramatic when a network is extremely sparse (left panels) and are more moderate for denser networks (right panels). Indeed, while the between-layer clustering of the layers is very accurate for $c = -0.05$, $d = 0.05$ if edges' signs are kept, it fails completely when these signs are removed. Moreover, even in the denser case, when $c = -0.2$, $d = 0.2$, the differences in clustering precision are very dramatic.

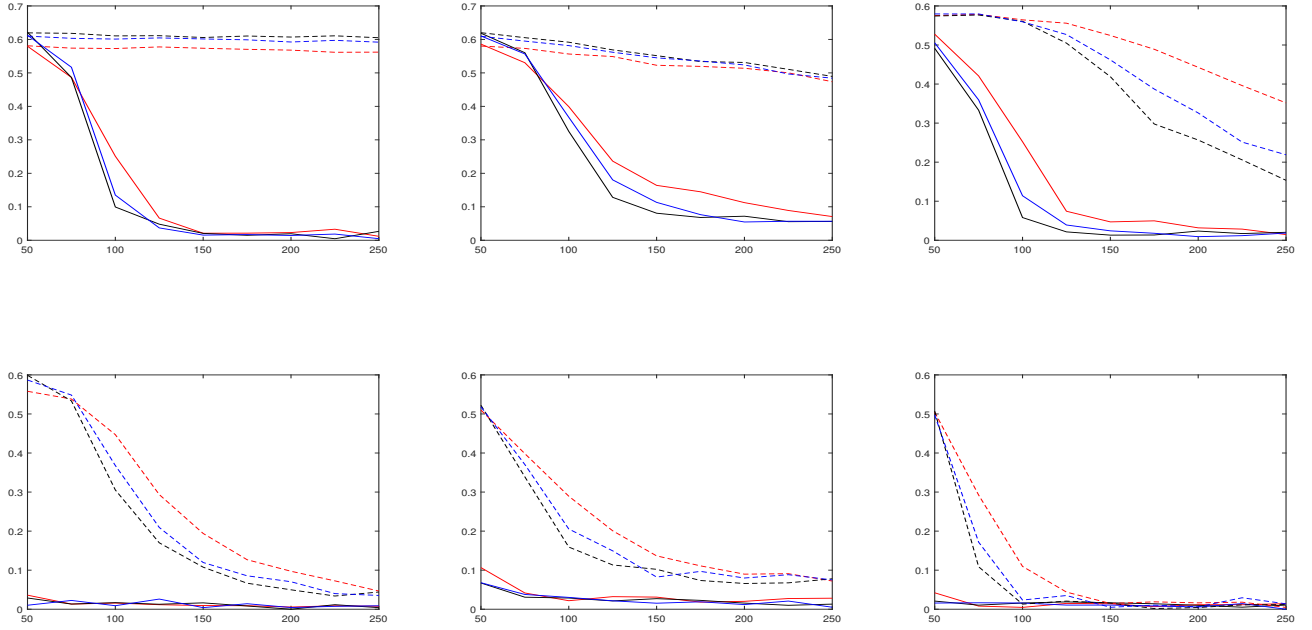


Fig. 3. Comparison of clustering errors when signs are present (solid lines) or removed (dash lines). The between-layer clustering errors R_{BL} in (28) of Algorithm 1 when matrices $X^{(m)}$ are generated by the truncated Dirichlet distribution with $M = 3$, $K_m = K = 3$, $\varpi_k = \alpha = 0.1$, $k \in [K + 1]$ (left panels). The between-layer clustering errors R_{BL} in (28) of Algorithm 1 (middle panels) and the within-layer clustering errors R_{WL} in (51) (right panel) when layers are equipped with the SBMs where matrices $X^{(m)}$, $m \in [M]$, are generated by the multinomial distribution with probabilities $(1/K_m, \dots, 1/K_m)$, $M = 3$ and $K_m = K = 3$. The entries of $B^{(l)}$ are generated as uniform random numbers between c and d with $c = -0.05$, $d = 0.05$ (top panels) and $c = -0.2$, $d = 0.2$ (bottom panels). Errors are averaged over 100 simulation runs, $L = 50$ (red), $L = 100$ (blue), $L = 150$ (black).

V. REAL DATA EXAMPLE

In this section we present an application of our model to the brain fMRI data set obtained from the Autism Brain Imaging Data Exchange (ABIDE I) located at

http://fcon_1000.projects.nitrc.org/indi/abide/abide_I.html

Specifically, we use 37 fMRI brain images obtained by California Institute of Technology and featured in [42]. The dataset contains resting-state fMRI data at the whole-brain level of 18 high-functioning adults with an Autism Spectrum Disorders (ASDs) and 19 neurotypical controls with no family history of autism, who were recruited under a protocol approved by the Human Subjects Protection Committee of the California Institute of Technology. The acquisition and initial processing of the data is described in [42], leading to a data matrix of the fMRI recordings over 116 brain regions (see, e.g., [40]) at 145 time instances.

The goal of our study was to create a signed multilayer network of brain connectivity, with layers being individuals, participating in the study, and to partition the layers of the network into groups using our methodology. We would like to point out that the objective of this example is illustration of our technique and of the advantage of keeping correlations' signs rather than in-depth investigation of brain networks associated with the ASDs. Since classification of noisy data without model selection is known to be as bad as pure guessing (see [16]), we further pre-processed the fMRI signals, using

wavelet denoising with the Daubechies-4 wavelets and soft thresholding to reduce noise and, subsequently, identified 64 brain regions by removing the regions that are not relates to cognitive functions. The necessity of removing irrelevant brain regions was motivated by the fact that vast majority of brain regions are not related to cognitive functions and therefore would make partitioning of layers of the network impossible (which was, in essence, the conclusion that [42] drew). Afterwards, for each individual, we created a signed network on the basis of pairwise correlations. Specifically, we used 40% of the highest correlations by absolute value, and created a signed adjacency tensor with values 0, 1 and -1. For the sake of comparison, we also created a corresponding adjacency tensor with signs removed.

Figure 4 pictures a brain network of one of the individuals in the study with signs (left panel) and sign-free (right panel). It is easy to see that negative and positive connections patterns are different, which helps to divide layers of the network into two groups. Specifically, on the average, networks have 1638.4 edges with 170 edges being negative. If we consider the two groups of layers (individuals with and without ASDs), the average numbers of edges are almost identical for the two groups (1638.4 for group 1 and 1638.5 for group 2), while the average number of negative edges exhibits a minor variation (173.0 for group 1 and 166.7 for group 2). Therefore, one cannot use the differences in the network densities for partitioning of layers into two groups, even if the signs of the

edges are taken into account.

In our analysis, we naturally used $M = 2$ (for individuals with and without ASDs), and chose $K = 4$. We scrambled the layers of the adjacency tensor and applied Algorithm 1 to its signed and signed-free versions. Since the results of the approximate k -means clustering are random, we repeated the process over 100 simulations runs. Thus, we obtained 18.9% average clustering error over signed multilayer network, and 35.2% if we ignore signs (with the standard deviations of about 0.6% in the signed network case and 2.7 % for the case without signs).

Finally, with an additional assumption that layers of the network follow the SBM, we partitioned the nodes in each of the two groups of layers into $K = 4$ communities. For this purpose, using Algorithm 2, we constructed estimators $\hat{V}_{1,S}, \hat{V}_{2,S}, \hat{V}_{1,NS}$ and $\hat{V}_{2,NS}$ for the the ambient subspace bases matrices $V_{1,S}, V_{2,S}, V_{1,NS}$ and $V_{2,NS}$, for the two groups of layers in the signed and sign-free cases, respectively. We carried out the k -means algorithm to partition rows of each of $\hat{V}_{1,S}, \hat{V}_{2,S}, \hat{V}_{1,NS}$ and $\hat{V}_{2,NS}$ into four communities and obtained four sets of community assignments, one for each of the two groups of layers and for the signed and the sign-free networks. Figure 5 presents components of the first two columns of $\hat{V}_{1,S}, \hat{V}_{2,S}$, and $\hat{V}_{1,NS}, \hat{V}_{2,NS}$, respectively, sorted by the assigned communities. In particular, Figure 5 confirms that keeping the signs of the edges leads to both more balanced communities and better community separation. Communities in Figure 5 are identified by different colors.

APPENDIX A APPENDIX. PROOFS

A. Proofs of Lemmas 1 and 2

Proof of Lemma 1. If $s(l_1) = m_1$ and $s(l_2) = m_2$, then, by (16), one has

$$\begin{aligned} \Theta(l_1, l_2) &= \left[\text{vec} \left(\tilde{U}^{(m_1)} (\tilde{U}^{(m_1)})^T \right) \right]^T \left[\text{vec} \left(\tilde{U}^{(m_2)} (\tilde{U}^{(m_2)})^T \right) \right] \\ &= \|\tilde{U}^{(m_1)} (\tilde{U}^{(m_2)})^T\|_F^2. \end{aligned}$$

Therefore, if $s(l_1) = s(l_2) = m$, then, $\Theta(l_1, l_2) = \|\tilde{U}^{(m)} (\tilde{U}^{(m)})^T\|_F^2 = \|I_{K_m}\|_F^2$, where I_k is the identity matrix of size k , and (18) holds. If $m_1 \neq m_2$, then, by (21), derive

$$\Theta(l_1, l_2) = \frac{\left\| \tilde{X}^{(m_1)} \left(\hat{\Sigma}^{(m_1)} \right)^{-\frac{1}{2}} \left[\tilde{X}^{(m_2)} \left(\hat{\Sigma}^{(m_2)} \right)^{-\frac{1}{2}} \right]^T \right\|_F^2}{(n-1)^2}.$$

Then, by Lemma 4, obtain that, if condition (91) holds, then, for $s(l_1) = m_1$ and $s(l_2) = m_2$, with probability at least $1 - 2Mn^{-\tau}$ one has one has

$$\max_{m_1 \neq m_2} |\Theta(l_1, l_2)| \leq 4 \underline{c}^{-2} (n-1)^{-2} \left\| \tilde{X}^{(m_1)} \left(\tilde{X}^{(m_2)} \right)^T \right\|_F^2.$$

Application of Lemma 5 and the fact that matrices $\tilde{X}^{(m)}$ have ranks at most K , yield that, with probability at least $1 - CMn^{-\tau}$, one has

$$\max_{l_1, l_2} |\Theta(l_1, l_2)| \leq CKn^{-1} \log n$$

which completes the proof of (19).

Proof of Lemma 2 Note that, for $l_1 \neq l_2$, one has

$$\begin{aligned} |(\hat{\theta}^{(l_1)})^T \hat{\theta}^{(l_2)} - (\theta^{(l_1)})^T \theta^{(l_2)}| &\leq |(\hat{\theta}^{(l_1)})^T [\hat{\theta}^{(l_2)} - \theta^{(l_2)}]| \\ &\quad + |[\hat{\theta}^{(l_1)} - \theta^{(l_1)}]^T \theta^{(l_2)}| \end{aligned}$$

Since $\|\theta^{(l)}\|^2 = K_m$ for $s(l) = m$, obtain

$$\begin{aligned} \max_{l_1, l_2} |(\hat{\theta}^{(l_1)})^T \hat{\theta}^{(l_2)} - (\theta^{(l_1)})^T \theta^{(l_2)}| \\ \leq \max_{l \in [L]} \|\hat{\theta}^{(l)} - \theta^{(l)}\| \left[2\sqrt{K_m} + \max_{l \in [L]} \|\hat{\theta}^{(l)} - \theta^{(l)}\| \right] \end{aligned}$$

Hence, due to

$$\begin{aligned} \|\hat{\theta}^{(l)} - \theta^{(l)}\| &= \left\| \hat{U}_A^{(l)} (\hat{U}_A^{(l)})^T - \tilde{U}_P^{(l)} (\tilde{U}_P^{(l)})^T \right\|_F \\ &= \sqrt{2} \left\| \sin \Theta(\hat{U}_A^{(l)}, \tilde{U}_P^{(l)}) \right\|_F \end{aligned}$$

and Lemma 6, derive $|(\hat{\theta}^{(l_1)})^T \hat{\theta}^{(l_2)} - (\theta^{(l_1)})^T \theta^{(l_2)}| \leq C\sqrt{K} (n\rho_n)^{-1/2} [2\sqrt{K} + C\sqrt{K} (n\rho_n)^{-1/2}]$, so that

$$\begin{aligned} \mathbb{P} \left\{ \max_{l_1, l_2} |(\hat{\theta}^{(l_1)})^T \hat{\theta}^{(l_2)} - (\theta^{(l_1)})^T \theta^{(l_2)}| \leq CK(n\rho_n)^{-\frac{1}{2}} \right\} \\ \geq 1 - 2n^{-(\tau-\tau_0)} \end{aligned} \quad (52)$$

Now, observe that, if $s(l_1) = s(l_2) = m$, then, due to $K_m \geq K/C_K$, $\Theta(l_1, l_2) = K_m$ and $\hat{\Theta}(l_1, l_2) \geq \Theta(l_1, l_2) - |(\hat{\theta}^{(l_1)})^T \hat{\theta}^{(l_2)} - (\theta^{(l_1)})^T \theta^{(l_2)}|$, one obtains (34) with probability at least $1 - 2n^{-(\tau-\tau_0)}$.

In order to derive (35), note that $\hat{\Theta}(l_1, l_2) \leq |\Theta(l_1, l_2)| + |(\hat{\theta}^{(l_1)})^T \hat{\theta}^{(l_2)} - (\theta^{(l_1)})^T \theta^{(l_2)}|$. Then (35) follows from the combination of (19) and (52) and the fact that $n^{-1} \log n = o((n\rho_n)^{-1/2})$ for large n .

B. Proofs of Theorems 1, 2 and 3

Proof of Theorem 1. Consider matrices $\mathcal{F} \in \mathbb{R}^{n^2 \times M}$ and $\Upsilon \in \mathbb{R}^{n^2 \times L}$ with rows $\mathcal{F}(m, :) = \text{vec}(U^{(m)}(U^{(m)})^T)$, $m \in [M]$, and $\Upsilon(l, :) = \text{vec}(U^{(l)}(U^{(l)})^T)$, $l \in [L]$, respectively. If S is the true clustering matrix and $W = SD_S^{-1/2}$, where $D_S = S^T S$, then

$$\Upsilon = S\mathcal{F} = WD_S^{1/2}, \quad \Theta = \Upsilon\Upsilon^T = WD_S^{1/2}\mathcal{F}\mathcal{F}^TD_S^{1/2}W^T.$$

Since Lemma 1 implies that

$$\begin{aligned} \lambda_{\min}(\mathcal{F}\mathcal{F}^T) &\geq \min_m K_m - CKM(n\rho_n)^{-1/2} \\ &\geq CK(1 - M(n\rho_n)^{-1/2}), \end{aligned}$$

obtain that, under assumption (36), one has

$$(dUp^2 = \sigma_{\min}^2(\Upsilon) = \lambda_{\min}(\Theta) \geq CKLM^{-1}). \quad (53)$$

Consider matrix $\hat{\Upsilon} \in \mathbb{R}^{n^2 \times L}$ with rows

$$\hat{\Upsilon}(l, :) = \text{vec}(\hat{U}^{(l)}(\hat{U}^{(l)})^T), \quad l \in [L].$$

Denote $\Xi = \hat{\Upsilon} - \Upsilon$ and observe that, by the Davis-Kahan theorem, with probability at least $1 - n^{-\tau}$, one has

$$\|\hat{\Upsilon} - \Upsilon\|_{2,\infty}^2 \asymp \max_{l \in [L]} \|\sin \Theta(\hat{U}^{(l)}, U^{(l)})\|_F^2 \leq \frac{C_\tau K^2 \log L}{n\rho_n}.$$

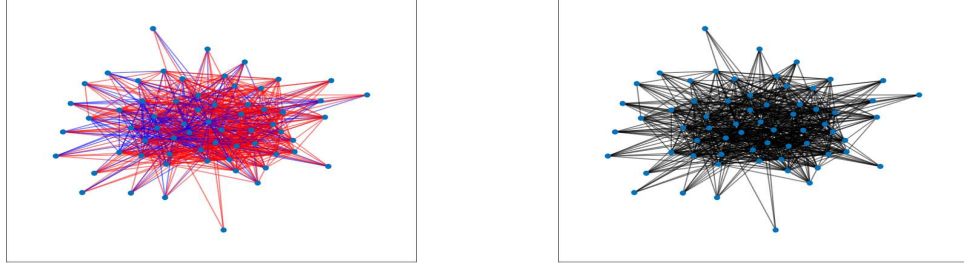


Fig. 4. The graphs of a network for brain regions of an individual with signs (left) and without signs (right). Positive edges are red, negative edges are blue. The networks are constructed using the brain fMRI data set obtained by the California Institute of Technology. Available as a part of the Autism Brain Imaging Data Exchange (ABIDE I) located at http://fcon_1000.projects.nitrc.org/indi/abide/abide_I.html

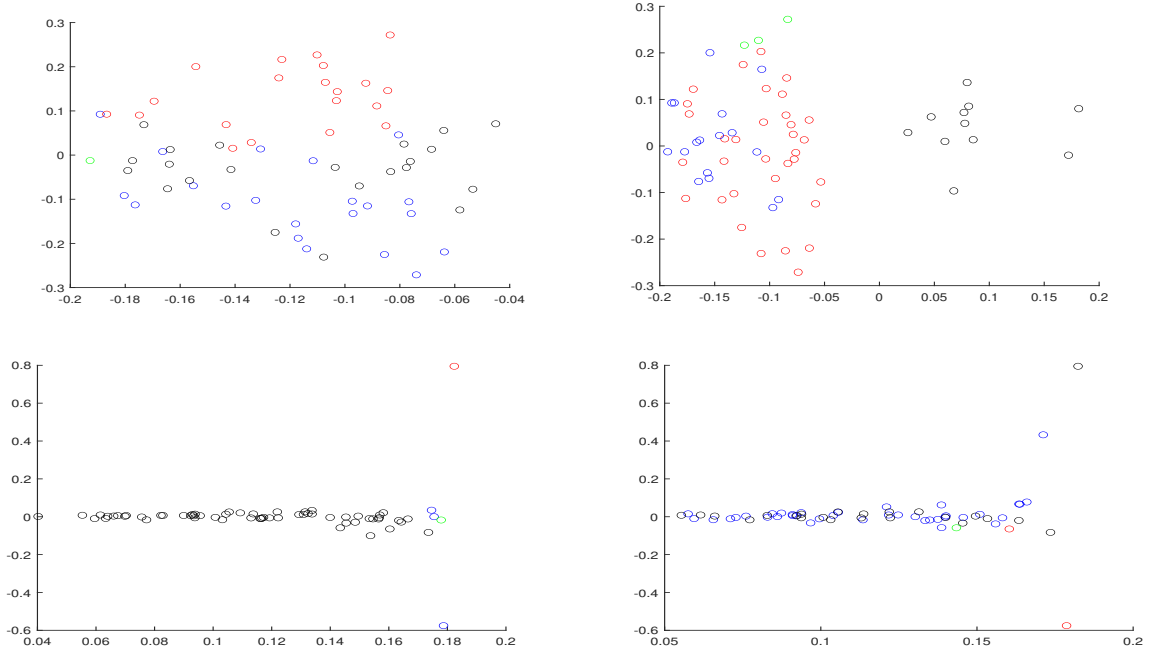


Fig. 5. The first two components of the eigenvectors, used for the community assignments in the two groups of layers of the multilayer network. Communities in the layers are identified by different colors. Top row: community assignments in the signed network. Bottom row: community assignments in the network with signs removed. Left column: group of layers 1, right column: group of layers 2. Networks are constructed using the brain fMRI data set obtained by the California Institute of Technology. Available as a part of the Autism Brain Imaging Data Exchange (ABIDE I) located at http://fcon_1000.projects.nitrc.org/indi/abide/abide_I.html

Hence, due to condition (10), with probability at least $1 - n^{-\tau}$, obtain

$$\begin{aligned} \|\Xi\|_{2,\infty} &\leq C_{\tau,\tau_0} K \sqrt{\log n} (n \rho_n)^{-1/2}, \\ \|\Xi\|_F &\leq C_{\tau,\tau_0} K \sqrt{L \log n} (n \rho_n)^{-1/2} \end{aligned} \quad (54)$$

Apply the second part of Proposition 1 of [36] with U being replaced by W , \hat{U} by \hat{W} , n by L , r by M , X by Υ , \hat{X} by $\hat{\Upsilon}$ and d_r by d_Υ . Consider the case of no hollowing, i.e., $\hat{h} = 0$, and define, similarly to [36],

$$\mathcal{E}_1 = \Xi \Xi^T, \quad \mathcal{E}_2 = \Xi \Upsilon^T, \quad \mathcal{E}_3 = \Upsilon \Xi^T, \quad \mathcal{E} = \mathcal{E}_1 + \mathcal{E}_2 + \mathcal{E}_3.$$

To apply Proposition 1 of [36], we need to check that, with probability at least $1 - n^{-\tau}$, one has $\sqrt{M} d_\Upsilon^{-2} \|\mathcal{E}\| = o(1)$ as

$n \rightarrow \infty$ and that conditions in formula (5.13) of Proposition 1 in [36] are valid. By observing that $\|\Upsilon\| \asymp d_\Upsilon$, derive that

$$d_\Upsilon^{-2} \|\mathcal{E}\| \leq d_\Upsilon^{-2} (\|\Xi\|^2 + 2 \|\Xi\| \|\Upsilon\|) \leq C d_\Upsilon^{-1} \|\Xi\| (1 + d_\Upsilon^{-1} \|\Xi\|)$$

Therefore, since $\|\Xi\| \leq \|\Xi\|_F$, obtain

$$\mathbb{P} \left\{ \frac{\|\Xi\|}{d_\Upsilon} \leq \frac{C_\tau \sqrt{K M \log n}}{\sqrt{n \rho_n}} \right\} \geq 1 - n^{-\tau}, \quad (55)$$

so that (36) guarantees that $\sqrt{M} d_\Upsilon^{-2} \|\mathcal{E}\| = o(1)$ as $n \rightarrow \infty$.

Now, we need to check that conditions in formula (5.13) of Proposition 1 in [36] hold. In our notations, the latter is true

if, with probability at least $1 - n^{-\tau}$, as $n \rightarrow \infty$, one has

$$\begin{aligned} L^{\frac{1}{2}} M^{-\frac{1}{2}} d_{\Upsilon}^{-2} \|\Xi \Xi^T W\|_{2,\infty} &\rightarrow 0, \\ L^{\frac{1}{2}} M^{-\frac{1}{2}} d_{\Upsilon}^{-2} \|\Xi \Upsilon^T W\|_{2,\infty} &\rightarrow 0, \\ L^{\frac{1}{2}} M^{-\frac{1}{2}} d_{\Upsilon}^{-2} \|\mathcal{E}_1 + \mathcal{E}_2\|_{2,\infty} &\rightarrow 0. \end{aligned} \quad (56)$$

We shall show that assumption (36) guarantees all of the statements in (56). It is easy to see that, by (53) and (54), one has

$$\frac{\|\Xi \Xi^T W\|_{2,\infty}}{d_{\Upsilon}^2} \leq \frac{\|\Xi\|_{2,\infty} \|\Xi\|}{d_{\Upsilon}^2} \leq C_{\tau} \frac{\sqrt{M} K \sqrt{M} \log n}{\sqrt{L} n \rho_n},$$

so that the first condition in (56) is ensured by (36). Similarly,

$$\frac{\|\Xi \Upsilon^T W\|_{2,\infty}}{d_{\Upsilon}^2} \leq \frac{C \|\Xi\|_{2,\infty}}{d_{\Upsilon}} \leq C_{\tau} \frac{\sqrt{M} \sqrt{K \log n}}{\sqrt{L} \sqrt{n \rho_n}},$$

so that the second condition in (56) is also ensured by (36). Finally, note that

$$\begin{aligned} d_{\Upsilon}^{-2} \|\mathcal{E}_1 + \mathcal{E}_2\|_{2,\infty} &\leq d_{\Upsilon}^{-1} \|\Xi\|_{2,\infty} (1 + d_{\Upsilon}^{-1} \|\Xi\|) \\ &\leq C_{\tau} \frac{\sqrt{M} K \log n \sqrt{M}}{\sqrt{L} n \rho_n}. \end{aligned}$$

Hence, the last condition in (56) is true, due to (36), so that the validity of Theorem 1 follows from Proposition 1 in [36].

Proof of Theorem 2 Fix $m \in [M]$ and consider $H^{(m)}$ and $\hat{H}^{(m)}$ defined in (24) and (26), respectively. Application of the Davis-Kahan theorem yields

$$\left\| \sin \Theta \left(\hat{U}^{(m)}, U^{(m)} \right) \right\| \leq \frac{C \|\hat{H}^{(m)} - H^{(m)}\|}{\sigma_{\min}(H^{(m)})} \quad (57)$$

Therefore, in order to assess $R_{U,\max}$ and $R_{U,\text{ave}}$, one needs to examine the spectral structure of matrices $H^{(m)}$ and their deviation from the sample-based versions $\hat{H}^{(m)}$. We start with the first task.

It follows from (7) and Assumption A5 that

$$(P^{(l)})^2 = \rho_n^2 X^{(m)} B_0^{(l)} (X^{(m)})^T X^{(m)} B_0^{(l)} (X^{(m)})^T \quad (58)$$

Recall that, by (12), $X^{(m)} = \tilde{X}^{(m)} + 1_n \bar{X}^{(m)}$, where $\tilde{X}^{(m)} = \Pi^{\perp} X^{(m)}$. Since $(\tilde{X}^{(m)})^T 1_n \bar{X}^{(m)} = 0$, by Lemma 2 of [8], obtain that $\sigma_{K_m}^2(X^{(m)}) \geq \sigma_{K_m}^2(\tilde{X}^{(m)})$. Furthermore, using (20) and Lemma 4, derive

$$\sigma_{K_m}^2(\tilde{X}^{(m)}) = \lambda_{\min}((\tilde{X}^{(m)})^T \tilde{X}^{(m)}) \geq \underline{c}n/4$$

The latter, together with (58) and Assumption A5, yields that

$$\sigma_{K_m}([P^{(l)}]^2) \geq \rho_n^2 \sigma_{K_m}^4(\tilde{X}^{(m)}) \sigma_{\min}^2(B_0^{(l)}) \geq C \rho_n^2 n^2.$$

Since matrices $[P^{(l)}]^2$ are all positive definite, one has $\sigma_{K_m}(H^{(m)}) \geq C L_m \rho_n^2 n^2$. Applying Lemma 3 with

$$1 + \log(n^{\tau}) / \log L \leq t \leq (\underline{c}_{\pi})^2 L / (2M^2 \log L) - 1, \quad (59)$$

and the union bound, derive from (90) that, with probability at least $1 - 2n^{-(\tau-\tau_0)}$

$$\min_m \sigma_{K_m}(H^{(m)}) \geq CLM^{-1} \rho_n^2 n^2. \quad (60)$$

Now, we examine deviations $\|\hat{H}^{(m)} - H^{(m)}\|^2$ in (57). Denote

$$\tilde{H}^{(m)} = \sum_{s(l)=m} \hat{G}^{(l)}, \quad \tilde{H}^{(m)} - H^{(m)} = \sum_{s(l)=m} [\hat{G}^{(l)} - G^{(l)}].$$

Observe that it follows from Theorem 4 of [31] and Theorem 1 that

$$\begin{aligned} \mathbb{P} \left\{ \|\tilde{H}^{(m)} - H^{(m)}\|^2 \leq C L_m (\rho_n^3 n^3 \log(n + L_m) + \rho_n^2 n^2) \right\} \\ \geq 1 - C n^{-(\tau-\tau_0)} - C(n + L_m)^{-(\tau-1)}. \end{aligned} \quad (61)$$

Now, recall that, by Theorem 1, with probability at least $1 - C n^{-(\tau-\tau_0)}$ one has $\hat{s} = s$, so that $\tilde{H}^{(m)} = \hat{H}^{(m)}$, $m \in [M]$. Hence, applying the union bound over $m \in [M]$ and combining (57), (60), Lemma 3 in Section A-D and (61), we arrive at

$$\max_{m \in [M]} \left\| \sin \Theta \left(\hat{U}^{(m)}, U^{(m)} \right) \right\| \leq C \left(\frac{\sqrt{M \log n}}{\sqrt{\rho_n n L}} + \frac{1}{n} \right) \quad (62)$$

with probability at least $1 - C n^{-(\tau-\tau_0)} - C M n^{-(\tau-1)}$, due to $\log(L_m + n) \propto \log(L + n) \propto \log n$. Now, in order the upper bound in (62) holds, one need the condition on t in (59) to be plausible, which is guaranteed by (38) and Assumption A4. The inequality (62) implies that in (32)

$$\mathbb{P} \left\{ R_{U,\max} \leq C_{\tau} \left(\frac{\sqrt{M \log n}}{\sqrt{\rho_n n L}} + \frac{1}{n} \right) \right\} \geq 1 - \frac{C}{n^{\tau-\tau_0-1}},$$

and that the first inequality in (39) holds. The validity of the second inequality follows from the fact that $R_{U,\text{ave}} \leq \sqrt{K} R_{U,\max}$.

Proof of Theorem 3 Note that validity of the Theorem follows immediately from Corollary 1. In order to prove (40), use Corollary 1 with $L = L_m$ for each of the groups of layers, and recall that $L_m \geq CL/M$ by Lemma 3. The proof is completed by application of the union bound.

C. Proofs of Corollaries 1 and 2

Proof of Corollary 1 Let assumptions of Theorem 2 hold with $M = 1$. the setting of the paper reduces to the COSIE model with $K_1 = K$. Denote

$$X = \sum_{l=1}^L (P^{(l)})^2, \quad \hat{X} = \sum_{l=1}^L [(A^{(l)})^2 - \hat{D}^{(l)}] \quad (63)$$

where $\hat{D}^{(l)}$ is defined in (25). Then, the SVDs of X and \hat{X} can be written, respectively, as

$$X = U \Psi U^T, \quad \hat{X} = \hat{U} \hat{\Psi} \hat{U}^T + \hat{U}_{\perp} \hat{\Psi}_{\perp} \hat{U}_{\perp}^T \quad (64)$$

where $U, \hat{U} \in \mathcal{O}_{n,K}$, $\hat{U}_{\perp} \in \mathcal{O}_{n,n-K}$ and $\hat{U}^T \hat{U}_{\perp} = 0$. Denote $\Xi^{(l)} = A^{(l)} - P^{(l)}$. Note that $\text{diag}(\hat{X}) = 0$, due to $(A^{(l)}(i, j))^2 = |A^{(l)}(i, j)|$. For any square matrix Y , denote $\mathcal{H}(Y) = Y - \text{diag}(Y)$, the so called hollowed matrix Y . With this notation, observe that $\hat{X} - X$ can be rewritten as

$$\Delta = \hat{X} - X = \mathcal{H}(\hat{X}) - X = \mathcal{H}(\hat{X} - X) - \text{diag}(X). \quad (65)$$

Hence, we can decompose the error as $\Delta = S_0 + S_1 + S_2$, where,

$$S_0 = \sum_{l=1}^L \mathcal{H} \left(P^{(l)} \Xi^{(l)} + \Xi^{(l)} P^{(l)} \right), \quad (66)$$

$$S_1 = \sum_{l=1}^L \mathcal{H} \left(\Xi^{(l)} \right)^2, \quad (67)$$

$$S_2 = - \sum_{l=1}^L \text{diag}(|X^{(l)}|), \quad (68)$$

Since Δ and X are the same as in Theorem 2, with probability at least $1 - C n^{-(\tau - (\tau_0 \vee 1))}$

$$\|\Delta\| \leq C \left[(\rho_n n)^{3/2} \sqrt{L \log n} + n \rho_n^2 L \right]. \quad (69)$$

Moreover, it is known that, for any square matrix Y

$$\|\mathcal{H}(Y)\| \leq 2\|Y\|. \quad (70)$$

In order to simplify the narrative, in what follows, we use C as a generic constant that depends only on the constants in our assumptions, C_τ as a generic constant that depends only on the constants in our assumptions and τ , and introduce a set $\Omega_{\tau,n}$, on which all inequalities take place, and such that

$$\mathbb{P}(\Omega_{\tau,n}) \geq 1 - C n^{-(\tau - (\tau_0 + 1))}. \quad (71)$$

For $\omega \in \Omega_{\tau,n}$, due to Assumptions **A2**, **A3** and **A5**, derive that

$$\lambda_{\min}(X) = \min_{i \in [K]} (\Psi_{i,i}) \geq C \rho_n^2 n^2 L. \quad (72)$$

Therefore, it follows from (33) and (69) that $\lambda_{\min}(\hat{\Psi}) \geq C \rho_n^2 n^2 L$ with probability at least $1 - C n^{-(\tau - (\tau_0 \vee 1))}$. As a result, for $\omega \in \Omega_{\tau,n}$ obtain

$$\|\hat{\Psi}^{-1}\| \leq C(\rho_n^2 n^2 L)^{-1}. \quad (73)$$

In addition, observe that by (21) and Lemma 4 with $M = 1$

$$\|U\|_{2,\infty} \leq C(K/n)^{1/2}. \quad (74)$$

Finally, combination of (69), (72) and Davis-Kahan theorem yields that, for $\omega \in \Omega_{\tau,n}$,

$$\|\sin \Theta(\hat{U}, U)\| \leq C \left[\frac{\sqrt{\log n}}{\sqrt{\rho_n n L}} + \frac{1}{n} \right]. \quad (75)$$

Let $U^T \hat{U} = U_H \Lambda_H V_H^T$ be the SVD of $U^T \hat{U}$. Denote $W_U = U_H V_H^T \in \mathcal{O}_K$. Instead of bounding above $R_{U,2,\infty}$, following [9], we bound $\|\hat{U} - UW_U\|_{2,\infty}$. For this purpose, we use Corollary 3.3 of [9] which states that

$$\begin{aligned} \hat{U} - UW_U &= (I - UU^T) \Delta U W_U \hat{\Psi}^{-1} \\ &\quad + (I - UU^T) \Delta (\hat{U} - UW_U) \hat{\Psi}^{-1} \\ &\quad + (I - UU^T) X (\hat{U} - UU^T \hat{U}) \hat{\Psi}^{-1} \\ &\quad + U(U^T \hat{U} - W_U). \end{aligned} \quad (76)$$

Due to (64), the third term in this expansion is equal to zero. Moreover, it is easy to see that

$$\sum_{l=1}^L (I - UU^T) P^{(l)} \Xi^{(l)} = 0,$$

so that one can replace S_0 in (66) by

$$\tilde{S}_0 = \sum_{l=1}^L \left[\Xi^{(l)} P^{(l)} - 2 \text{diag}(\Xi^{(l)} P^{(l)}) \right]. \quad (77)$$

After that, replace Δ by $S = \tilde{S}_0 + S_1 + S_2$, and obtain from (76) that

$$R = \|\hat{U} - UW_U\|_{2,\infty} \leq R_1 + R_2 + R_3 + R_4 + R_5 \quad (78)$$

with

$$\begin{aligned} R_1 &= \|U\|_{2,\infty} \|SU\| \|\hat{\Psi}^{-1}\|, \\ R_2 &= \|SU\|_{2,\infty} \|\hat{\Psi}^{-1}\|, \\ R_3 &= \|U\|_{2,\infty} \|S\| \|\hat{U} - UW_U\| \|\hat{\Psi}^{-1}\|, \\ R_4 &= \|S\|_{2,\infty} \|\hat{U} - UW_U\| \|\hat{\Psi}^{-1}\|, \\ R_5 &= \|U\|_{2,\infty} \|(U^T \hat{U} - W_U)\|. \end{aligned}$$

It follows from (107) of Lemma 7, and [9] that

$$\begin{aligned} \|\hat{U} - UW_U\| &\leq \sqrt{2} \|\sin \Theta(\hat{U}, U)\|, \\ \|(U^T \hat{U} - W_U)\| &\leq \|\sin \Theta(\hat{U}, U)\|^2. \end{aligned}$$

Note that

$$\begin{aligned} \|\tilde{S}_0\| &\leq \left\| \sum_{l=1}^L \Xi^{(l)} P^{(l)} \right\| + 2 \left\| \text{diag} \left(\sum_{l=1}^L \Xi^{(l)} P^{(l)} \right) \right\| \\ &\leq 3 \left\| \sum_{l=1}^L \Xi^{(l)} P^{(l)} \right\|. \end{aligned}$$

Then, by the same argument that was used to obtain the upper bound for $\|S_0\|$, obtain that, for $\omega \in \Omega_{\tau,n}$,

$$\|\tilde{S}_0\| \leq C_\tau (\rho_n^3 n L \log L)^{1/2}.$$

Since $\|S_1\|$ and $\|S\|_2$ have the same upper bounds as before (up to a constant), derive that

$$\|S\| \leq C \left[(\rho_n n)^{3/2} \sqrt{L \log n} + n \rho_n^2 L \right]. \quad (79)$$

Denote

$$\epsilon_{\rho,n} = (\rho_n n L)^{-1/2} (\log n)^{1/2} + n^{-1} \quad (80)$$

and observe that

$$\begin{aligned} \|S\| \|\hat{\Psi}^{-1}\| &\leq C_\tau \epsilon_{\rho,n}, \quad \|\hat{U} - UW_U\| \leq C_\tau \epsilon_{\rho,n}, \\ \|(U^T \hat{U} - W_U)\| &\leq C_\tau \epsilon_{\rho,n}. \end{aligned} \quad (81)$$

Then, we need to obtain upper bounds for $\|SU\|$, $\|SU\|_{2,\infty}$ and $\|S\|_{2,\infty}$. Due to $S = \tilde{S}_0 + S_1 + S_2$, we develop those bounds for \tilde{S}_0 , S_1 and S_2 , separately.

Bounds for the norms of \tilde{S}_0 . In order to derive upper bounds for $\|\tilde{S}_0 U\|_{2,\infty}$ and $\|\tilde{S}_0\|_{2,\infty}$, denote $\xi^{(i,l)} := \Xi^{(l)}(:, i)$, $i \in [n]$, and observe that, due to symmetry,

$$\|\tilde{S}_0 U\|_{2,\infty} \leq \|\tilde{S}_0 U\|_{2,\infty} = \max_{i \in [n]} \left\| \sum_{l=1}^L P^{(l)} \xi^{(i,l)} \right\|.$$

Here, for a fixed value of i , components of vectors $\xi^{(i,l)}$ are independent Bernoulli errors, and application of Theorem 3 of

[31] with $j = 0, 1$, in a view of $\sum_{l=1}^L \|P^{(l)}\|_F^2 \leq C\rho_n^2 n^2 L$ and $\max_l \|P^{(l)}\|_{2,\infty} \leq C\rho_n \sqrt{n}$, yields

$$\mathbb{P} \left\{ \left\| \sum_{l=1}^L P^{(l)} \xi^{(i,l)} \right\| \geq t \right\} \leq 2(n+1) \left[\exp \left(-\frac{ct^2}{Ln^2 \rho_n^3} \right) + \exp \left(-\frac{Ct}{\rho_n \sqrt{n}} \right) \right].$$

Set $t = C_\tau \sqrt{\rho_n^3 n^2 L \log n}$. Then, taking a union bound over $i \in [n]$ and choosing an appropriate constant C_τ , which depends on τ , derive that, for $\omega \in \Omega_{\tau,n}$,

$$\|\tilde{S}_0 U\|_{2,\infty} \leq \|\tilde{S}_0\|_{2,\infty} \leq C \sqrt{\rho_n^3 n^2 L \log n}. \quad (82)$$

Bounds for the norms of S_1 . Let $\xi^{(i,l)} := \Xi^{(l)}(:, i)$, as before. Consider matrices $\Xi_{(-i)}^{(l)} \in \mathbb{R}^{n \times n}$, where the i -th row and the i -th column are replaced by zeros. It is easy to see that for any i and l , vectors $\xi^{(i,l)}$ and matrices $\Xi_{(-i)}^{(l)}$ are independent. Observe also that

$$S_1(i, :) = \sum_{l=1}^L \left[(\xi^{(i,l)})^T \Xi_{(-i)}^{(l)} + \Xi^{(l)}(i, i) (\xi^{(i,l)})^T \right].$$

Since $A^{(l)}(:, i) = 0$, one has $\Xi^{(l)}(i, i) = -P^{(l)}(i, i)$, so that, for $j = 0, 1$, one has

$$S_1(i, :) U^j = \sum_{l=1}^L \left[(\xi^{(i,l)})^T \Xi_{(-i)}^{(l)} U^j - P^{(l)}(i, i) (\xi^{(i,l)})^T U^j \right].$$

Note that, for $\omega \in \Omega_{\tau,n}$ and $j = 0, 1$, one has

$$\max_{i \in [n]} \left\| \sum_{l=1}^L P^{(l)}(i, i) (\xi^{(i,l)})^T U^j \right\| \leq C_\tau \sqrt{\rho_n^3 n L \log n}. \quad (83)$$

Therefore, due to symmetry, obtain, for $\omega \in \Omega_{\tau,n}$ and $j = 0, 1$,

$$\|S_1 U^j\|_{2,\infty} \leq \max_{i \in [n]} \left\| \sum_{l=1}^L (\xi^{(i,l)})^T \Xi_{(-i)}^{(l)} U^j \right\| + C_\tau \sqrt{\rho_n^3 n L \log n}.$$

In order to obtain an upper bound for the first term in the last inequality, apply Theorem 3 of [31] with $j = 0, 1$, conditional on $\Xi_{(-i)}^{(l)}$, $l \in [L]$. Obtain

$$\mathbb{P} \left\{ \left\| \sum_{l=1}^L (\xi^{(i,l)})^T \Xi_{(-i)}^{(l)} U^j \right\| \geq t \mid \Xi_{(-i)}^{(l)}, l \in [L] \right\} \leq 2(n+1) \left\{ \exp \left(-\frac{t^2}{8\rho_n \Delta_1(j)} \right) + \exp \left(-\frac{t}{4\Delta_2(j)} \right) \right\}, \quad (84)$$

where

$$\Delta_1(j) = \sum_{l=1}^L \|\Xi_{(-i)}^{(l)} U^j\|_F^2, \quad \Delta_2(j) = \max_{l \in [L]} \|\Xi_{(-i)}^{(l)} U^j\|_{2,\infty}.$$

The upper bounds for the above quantities are provided by Lemma 8, formally stated and proved in the next section.

Specifically, Lemma 8 implies that, with probability at least $1 - C n^{-(\tau - (\tau_0 \vee 1))}$,

$$\max(\Delta_1(0), \Delta_1(1)) \leq C_\tau \sqrt{n \rho_n \log n}, \\ \Delta_2(0) \leq C_\tau \rho_n n^2 L, \quad \Delta_2(1) \leq C_\tau \rho_n n K L.$$

Plug those quantities into (84) and set $t = t_0$ and $t = t_1$ for $j = 0$ and $j = 1$, respectively, where

$$t_0 = C_\tau \sqrt{\rho_n^2 n^2 L}, \quad t_1 = C_\tau \sqrt{\rho_n^2 n K L}.$$

Obtain that, for $\omega \in \Omega_{\tau,n}$,

$$\|S_1\|_{2,\infty} \leq C_\tau \sqrt{\rho_n^2 n^2 L}, \quad \|S_1 U\|_{2,\infty} \leq C_\tau \sqrt{\rho_n^2 n K L}. \quad (85)$$

Bounds for the norms of S_2 . Since S_2 is the diagonal matrix, obtain that $\|S_2\|_{2,\infty} = \|S_2\|_{1,\infty} = \|S_2\|$, and it follows from Proposition 6.5 of [9] that

$$\|S_2\|_{2,\infty} \leq C_\tau \rho_n^2 n L, \quad \|S_2 U\|_{2,\infty} \leq C_\tau \rho_n^2 \sqrt{n K L}. \quad (86)$$

Overall upper bounds. Now, from (82), (85) and (86), for $\omega \in \Omega_{\tau,n}$, obtain that

$$\|S\|_{2,\infty} \leq C_\tau \left[\sqrt{\rho_n^2 n^2 L} + \rho_n^2 n L \right], \\ \|S U\|_{2,\infty} \leq C_\tau \left[\sqrt{\rho_n^3 n^2 L \log n} + \sqrt{\rho_n^2 n K L} + \rho_n^2 \sqrt{n K L} \right],$$

Therefore, (73) yields

$$\|S\|_{2,\infty} \|\hat{\Psi}^{-1}\| \leq C_\tau \left[\frac{\sqrt{\log n}}{\rho_n n \sqrt{L}} + \frac{1}{n} \right], \quad (87)$$

$$\|S U\|_{2,\infty} \|\hat{\Psi}^{-1}\| \leq C_\tau \left[\frac{\sqrt{K} \epsilon_{\rho,n}}{\sqrt{n}} + \frac{\sqrt{\log n}}{\sqrt{n} \sqrt{\rho_n n L}} \right], \quad (88)$$

where $\epsilon_{\rho,n}$ is defined in (80).

Hence, using (81), (74), (87) and (88), and the fact that the second term in (88) is asymptotically smaller than the first, we obtain upper bounds for the components R_i , $i \in [5]$, of R in (78):

$$R_1 \leq C_\tau K^{1/2} n^{-1/2} \epsilon_{\rho,n}, \\ R_2 \leq C_\tau K^{1/2} n^{-1/2} \epsilon_{\rho,n}, \\ R_3 \leq C_\tau K^{1/2} n^{-1/2} \epsilon_{\rho,n}^2, \\ R_4 \leq C_\tau [n^{-1} + (\rho_n n)^{-1} L^{-1/2} (\log n)^{1/2}] \epsilon_{\rho,n}, \\ R_5 \leq C_\tau K^{1/2} n^{-1/2} \epsilon_{\rho,n}^2.$$

Since $\epsilon_{\rho,n} = o(1)$, we arrive at (41).

Proof of Corollary 2 Validity of Corollary 2 follows directly from Theorem 1.

D. Proofs of supplementary statements

Lemma 3. Let Assumption A1 hold. Denote

$$L_m = \sum_{l=1}^M I(s(l) = m), \quad m \in [M]. \quad (89)$$

If $t \leq (\underline{c}_\pi)^2 L / (2M^2 \log L) - 1$, then,

$$\mathbb{P} \left\{ \bigcap_{m=1}^M \left(\frac{\underline{c}_\pi L}{2M} \leq L_m \leq \frac{3\bar{c}_\pi L}{2M} \right) \right\} \geq 1 - 2L^{-t}. \quad (90)$$

Proof of Lemma 3. Note that $L_m \sim \text{Binomial}(\pi_m, L)$ for a fixed m . By Hoeffding inequality, for any $x > 0$

$$\mathbb{P}\{|L_m/L - \pi_m| \geq x\} \leq 2\exp\{-2Lx^2\}$$

Then, applying Assumption A1 and the union bound, obtain

$$\mathbb{P}\left\{\bigcap_{m=1}^M (\underline{c}_\pi L/M - Lx \leq L_m \leq \bar{c}_\pi L/M + Lx)\right\} \geq 1 - 2M \exp\{-2Lx^2\}$$

Now, set $x = \sqrt{\log(L^t M)/(2L)}$, which is equivalent to $M \exp\{-2Lx^2\} = L^{-t}$. If let L is large enough, so that $x < \underline{c}_\pi/(2M)$, then (90) holds. The latter is guaranteed by $t+1 \leq (\underline{c}_\pi)^2 L/(2M^2 \log L)$.

Lemma 4. Let Assumptions A1–A4 hold. Let n be large enough, so that

$$n \geq 2(C_\tau)^2 (\bar{c})^2 (\underline{c})^{-4} (K + \tau \log n) \quad (91)$$

where C_τ is the constant in (93) Then, for any fixed constant τ , one has

$$\mathbb{P}\left\{\min_{m \in [M]} \lambda_{\min}(\widehat{\Sigma}^{(m)}) \geq \frac{\underline{c}}{2}\right\} \geq 1 - 2Mn^{-\tau} \quad (92)$$

Proof of Lemma 4. Apply Theorem 6.5 of [43] which states that, under conditions of the Lemma, with probability at least $1 - 2n^{-\tau}$, one has

$$\|\widehat{\Sigma}^{(m)} - \Sigma^{(m)}\| \leq \frac{C_\tau \bar{c}}{\underline{c}} \sqrt{\frac{K + \tau \log n}{n}}. \quad (93)$$

Since $\lambda_{\min}(\widehat{\Sigma}^{(m)}) \geq \lambda_{\min}(\Sigma^{(m)}) - \|\widehat{\Sigma}^{(m)} - \Sigma^{(m)}\|$, by Assumption A3, obtain that, with probability at least $1 - 2n^{-\tau}$

$$\lambda_{\min}(\widehat{\Sigma}^{(m)}) \geq \underline{c} \left[1 - \frac{C_\tau \bar{c}}{\underline{c}^2} \sqrt{\frac{K + \tau \log n}{n}}\right]. \quad (94)$$

If n satisfies (91), the expression in the square brackets in (94) is bounded below by $1/2$ and, by taking the union bound in (94), we complete the proof.

Lemma 5. Let Assumptions A1–A4 hold. Then, for any fixed constant τ , one has

$$\mathbb{P}\left\{\max_{i \neq j} \|(\tilde{X}^{(i)})^T \tilde{X}^{(j)}\| \leq C_1 \sqrt{n \log n}\right\} \geq 1 - C_2 n^{-\tau}, \quad (95)$$

where C_1 and C_2 in (95) depend on τ and constants in Assumptions A1–A4 only.

Proof of Lemma 5. Note that $\tilde{X}^{(i)} = X^{(i)} - \Pi X^{(i)} = (X^{(i)} - 1_n \mu^{(i)}) + (1_n \mu^{(i)} - \Pi X^{(i)})$. Introduce matrices

$$\xi^{(i)} = X^{(i)} - 1_n \mu^{(m_i)}, \quad \eta^{(i)} = 1_n \mu^{(i)} - \Pi X^{(i)}, \quad (96)$$

$$\xi^{(i)}, \eta^{(i)} \in \mathbb{R}^{n \times K_i}, \quad i \in [M]$$

Observe that, by (6), one has $\mathbb{E}\xi^{(i)} = \mathbb{E}\eta^{(i)} = 0$ and that pairs $(\xi^{(i)}, \eta^{(i)})$ and $(\xi^{(j)}, \eta^{(j)})$ are independent for $i \neq j$. Note also that

$$\Delta^{(i,j)} = \|(\tilde{X}^{(i)})^T \tilde{X}^{(j)}\| \leq \Delta_1^{(i,j)} + \Delta_2^{(i,j)} + \Delta_3^{(i,j)} + \Delta_4^{(i,j)},$$

where $\Delta_1^{(i,j)} = \|(\xi^{(i)})^T \xi^{(j)}\|$, $\Delta_2^{(i,j)} = \|(\xi^{(i)})^T \eta^{(j)}\|$, $\Delta_3^{(i,j)} = \|(\eta^{(i)})^T \xi^{(j)}\|$ and $\Delta_4^{(i,j)} = \|(\eta^{(i)})^T \eta^{(j)}\|$. Below, we construct upper bounds for Δ_k , $k = 1, 2, 3, 4$.

An upper bound for $\Delta_1^{(i,j)}$. Define matrix $\Psi = (\xi^{(i)})^T \xi^{(j)} \in \mathbb{R}^{K_i \times K_j}$ and note that

$$\Psi = \sum_{t=1}^n \Psi_t, \quad \Psi_t = (\xi^{(i)}(t, :))^T \xi^{(j)}(t, :), \quad \mathbb{E}\Psi_t = 0,$$

where rank one matrices Ψ_t are i.i.d. for different values of $t \in [n]$. We apply matrix Bernstein inequality from [41]

$$\mathbb{P}\{\|\Psi\| \geq z\} \leq (K_i + K_j) \exp\left\{-\frac{z^2}{2(n\delta_1 + z\delta_2/3)}\right\}, \quad (97)$$

with $\delta_1 = \max[\|\mathbb{E}(\Psi_1 \Psi_1^T)\|, \|\mathbb{E}(\Psi_1^T \Psi_1)\|]$ and $\delta_2 = \max_t \|\Psi_t\|$. It is easy to see that $\delta_2 = \|\xi^{(i)}(t, :)\| \|\xi^{(j)}(t, :)\| \leq 1$ by Assumption A2. In order to upper-bound δ_1 , note that

$$\begin{aligned} \mathbb{E}(\Psi_1 \Psi_1^T) &= \mathbb{E}\|\xi^{(j)}(t, :)\|^2 \mathbb{E}\left[(\xi^{(i)}(1, :))^T \xi^{(i)}(1, :)\right] \\ &\leq \mathbb{E}\left[(\xi^{(i)}(1, :))^T \xi^{(i)}(1, :)\right] \end{aligned}$$

and, by (6), $\mathbb{E}\left[(\xi^{(i)}(1, :))^T \xi^{(i)}(1, :)\right] = \Sigma^{(i)}$. Therefore, $\|\mathbb{E}(\Psi_1 \Psi_1^T)\| \leq \bar{c}$. Similarly,

$$\begin{aligned} \mathbb{E}(\Psi_1^T \Psi_1) &= \mathbb{E}\left[\xi^{(i)}(1, :)\mathbb{E}\left((\xi^{(j)}(1, :))^T \xi^{(j)}(1, :)\right)(\xi^{(i)}(1, :))^T\right] \\ &= \mathbb{E}\left[\xi^{(i)}(1, :)\Sigma^{(j)}(\xi^{(i)}(1, :))^T\right] \end{aligned}$$

and, hence

$$\|\mathbb{E}(\Psi_1^T \Psi_1)\| \leq \bar{c} \mathbb{E}\|\xi^{(i)}(1, :)\|^2 \leq \bar{c}$$

Therefore, combination of (97) and the union bound over $i, j \in [M]$ yield, for any $\tau > 0$,

$$\mathbb{P}\left\{\max_{i \neq j} \Delta_1^{(i,j)} \leq C \sqrt{n \log(M^2 n)}\right\} \geq 1 - n^{-\tau}. \quad (98)$$

Now, consider $\Delta_2^{(i,j)} = \|(\xi^{(i)})^T \eta^{(j)}\|$. Observe that, due to $n^{-1} 1_n^T X^{(i)} = \bar{X}^{(i)}$, one has

$$\begin{aligned} (\xi^{(i)})^T \eta^{(j)} &= (X^{(i)} - 1_n \mu^{(m_i)})^T (1_n \mu^{(j)} - \Pi X^{(j)}) \\ &= n(\bar{X}^{(i)} - \mu^{(i)})^T (\bar{X}^{(j)} - \mu^{(j)}), \end{aligned}$$

and a similar calculation applies to $(\eta^{(i)})^T \xi^{(j)}$ and $(\eta^{(i)})^T \eta^{(j)}$. Therefore, for $i, j \in [M]$

$$\Delta_k^{(i,j)} \leq n \|\bar{X}^{(i)} - \mu^{(i)}\| \|\bar{X}^{(j)} - \mu^{(j)}\|, \quad k = 2, 3, 4. \quad (99)$$

It is known (see, e.g., [43]) that if ζ is a zero mean sub-gaussian k -dimensional random vector with the sub-gaussian parameter σ , then

$$\mathbb{P}\left\{\|\zeta\| \leq 4\sigma\sqrt{k} + 2\sigma\sqrt{\log(1/\epsilon)}\right\} \geq 1 - \epsilon. \quad (100)$$

Note that vectors $(\Sigma^{(i)})^{-1/2} (X(j, :) - \mu^{(i)})$ are anisotropic K_i dimensional random vectors of length at most $1/\sqrt{\underline{c}}$. Hence,

vectors $(\Sigma^{(i)})^{-1/2} (\bar{X}^{(i)} - \mu^{(i)})$ are anisotropic sub-gaussian with $\sigma \leq 2/\sqrt{\underline{c}n}$, so that

$$\mathbb{P} \left\{ \|\bar{X}^{(i)} - \mu^{(i)}\| \leq \frac{4\sqrt{\underline{c}}[2\sqrt{K} + \sqrt{\log(M^2 n^\tau)}]}{\sqrt{n\underline{c}}} \right\} \geq 1 - M^{-2} n^{-\tau}. \quad (101)$$

Combining (99), (101) and the union bound over $i, j \in [M]$, $i \neq j$, obtain, for $k = 2, 3, 4$:

$$\mathbb{P} \left\{ \max_{i \neq j} \Delta_k^{(i,j)} \leq C \sqrt{K + \log(M^2 n)} \right\} \geq 1 - n^{-\tau}, \quad (102)$$

which, together with (98) and $\log(M^2 n) \propto \log n$, complete the proof.

Lemma 6. *Let Assumptions A1–A5 and (33) hold. Then, if n is large enough, for any fixed constant τ , with probability at least $1 - 2n^{-(\tau-\tau_0)}$, one has*

$$\max_{l \in [L]} \left\| \sin \Theta(\tilde{U}_A^{(l)}, \tilde{U}_P^{(l)}) \right\|_F \leq C K^{1/2} (n\rho_n)^{-1/2}. \quad (103)$$

Proof of Lemma 6. It follows from [30] that, under condition (33), one has

$$\mathbb{E} \|A^{(l)} - P^{(l)}\| \leq C \left(\sqrt{n\rho_n} + \sqrt{\log n} \right).$$

Also, by formula (2.4) of [7], derive that, for any $t > 0$, and some absolute constant \tilde{C} one has

$$\mathbb{P} \left\{ \|A^{(l)} - P^{(l)}\| - \mathbb{E} \|A^{(l)} - P^{(l)}\| \geq t \right\} \leq 2 \exp(-\tilde{C} t^2).$$

Setting $t = \sqrt{\tilde{C}^{-1} \log(n^\tau L)}$, combining the two inequalities above and applying the union bound, obtain

$$\mathbb{P} \left\{ \|A^{(l)} - P^{(l)}\| \leq C \left(\sqrt{n\rho_n} + \sqrt{\log(n^\tau L)} \right) \right\} \geq 1 - 2n^{-\tau}, \quad (104)$$

where the constant C in (104) depends on τ and the constants in Assumptions A1–A5. Taking into account that $\|\tilde{A}^{(l)} - \tilde{P}^{(l)}\| \leq \|A^{(l)} - P^{(l)}\|$ and that, under assumptions of the Lemma, $\log(n^\tau L) \leq C \log n \leq Cn\rho_n$, derive that

$$\mathbb{P} \left\{ \|\tilde{A}^{(l)} - \tilde{P}^{(l)}\| \leq C\sqrt{n\rho_n} \right\} \geq 1 - 2n^{-\tau}. \quad (105)$$

By Davis-Kahan Theorem (see, e.g., [44]), if $s(l) = m$, obtain

$$\left\| \sin \Theta(\tilde{U}_A^{(l)}, \tilde{U}_P^{(l)}) \right\|_F \leq \frac{2\sqrt{K_m} \|\tilde{A}^{(l)} - \tilde{P}^{(l)}\|}{\sigma_{K_m}(\tilde{P}^{(l)})}. \quad (106)$$

Here, by (13) and (14), $\tilde{P}^{(l)} = \tilde{X}^{(m)} B^{(l)} (\tilde{X}^{(m)})^T = \rho_n \tilde{U}^{(m)} \tilde{D}^{(m)} (\tilde{O}^{(m)})^T B_0^{(l)} (\tilde{D}^{(m)} (\tilde{O}^{(m)})^T)^T (\tilde{U}^{(m)})^T$, so that, by (20),

$$\tilde{P}^{(l)} = (n-1) \rho_n \tilde{U}^{(m)} \sqrt{\hat{\Sigma}^{(m)}} B_0^{(l)} (\sqrt{\hat{\Sigma}^{(m)}})^T (\tilde{U}^{(m)})^T.$$

Therefore, Assumption A5 and Lemma 4 imply that

$$\sigma_{K_m}(\tilde{P}^{(l)}) \geq Cn\rho_n$$

Combining the latter with (105) and (106), using the union bound over $l \in [L]$, and taking into account that $K_m \leq K$, obtain (103).

Lemma 7. *Let $\tilde{H} = U_H \Lambda_H V_H^T$ be the SVD of $\tilde{H} = U^T \hat{U}$. Denote $W_U = U_H V_H^T \in \mathcal{O}_K$. Then,*

$$\|U^T \hat{U} - W_U\| \leq \|\sin \Theta(U, \hat{U})\|^2. \quad (107)$$

Proof of Lemma 7. Observe that $\Lambda_H = \cos(\Theta)$, where Θ is the diagonal matrix of the principal angles between the subspaces. Therefore, due to inequality $\sin(\theta/2) \leq \sin \theta / \sqrt{2}$ for $0 \leq \theta \leq \pi/2$, one has

$$\begin{aligned} \|W_U - \tilde{H}\| &= \|U_H (\cos \Theta - I_K) V_H^T\| = 2 \|\sin^2(\Theta/2)\| \\ &\leq \|\sin \Theta\|^2 = \|\sin \Theta(U, \hat{U})\|^2. \end{aligned}$$

Lemma 8. *Let assumptions of Theorem 2 hold with $M = 1$. Then, for any $\tau > 0$, and absolute constant C_τ that depends on τ and constants in Assumptions A1–A5 only, with probability at least $1 - Cn^{-(\tau-(\tau_0+1))}$, one has for $j = 0, 1$*

$$\max_{l \in [L]} \max_{j=0,1} \|\Xi^{(l)} U^j\|_{2,\infty} \leq C_\tau \sqrt{n\rho_n \log n}, \quad (108)$$

$$\sum_{l=1}^L \|\Xi^{(l)}_{(-i)}\|_F^2 \leq C_\tau \rho_n n^2 L, \quad (109)$$

$$\sum_{l=1}^L \|\Xi^{(l)}_{(-i)} U\|_F^2 \leq C_\tau \rho_n n K L. \quad (110)$$

Proof of Lemma 8. Note that the first inequality follows from Theorem 5.2 of [32] and the fact that

$$\|\Xi^{(l)} U^j\|_{2,\infty} \leq \|\Xi^{(l)}\| \|U^j\| \leq \|\Xi^{(l)}\|.$$

In order to prove (109), note that

$$\mathbb{E} \left(\sum_{l=1}^L \|\Xi^{(l)}\|_F^2 \right) \leq L n^2 \rho_n \quad (111)$$

Furthermore, introduce random variables $\eta_{i,j}^{(l)} = [\Xi^{(l)}(i, j)]^2 - \mathbb{E} [\Xi^{(l)}(i, j)]^2$. Observe that $\eta_{i,j}^{(l)}$ are independent zero mean random variables, for $1 \leq i \leq j \leq n$ and $l \in [L]$, with $|\eta_{i,j}^{(l)}| \leq 1$ and $\text{Var}(\eta_{i,j}^{(l)}) \leq \rho_n$. Then, application of the Bernstein inequality yields

$$\mathbb{P} \left\{ \sum_{l=1}^L \sum_{1 \leq i \leq j \leq n} \eta_{i,j}^{(l)} \geq t_1 \right\} \leq 2 \exp \left(-\frac{C t_1^2}{L n^2 \rho_n} \right) + 2 \exp(-C t_1).$$

Setting $t_1 = C_\tau \sqrt{\rho_n n^2 L \log n}$ and taking into account (111), obtain, with probability at least $1 - Cn^{-\tau}$, that

$$\sum_{l=1}^L \|\Xi^{(l)}_{(-i)}\|_F^2 \leq L n^2 \rho_n + C_\tau \sqrt{\rho_n n^2 L \log n}.$$

Then, (109) follows from the fact that, in the last inequality, the first term dominates the second, and from the fact that $\|\Xi^{(l)}_{(-i)}\|_F^2 \leq \|\Xi^{(l)}\|_F^2$.

In order to assert the validity of (110), observe that $\text{rank}(\Xi^{(l)}_{(-i)} U) \leq K$, and, therefore, by Theorem 5.2 of [32], derive

$$\|\Xi^{(l)}_{(-i)} U\|_F^2 \leq C K \|\Xi^{(l)}\|^2 \leq C K n \rho_n.$$

ACKNOWLEDGMENT

The author of the paper gratefully acknowledges partial support by National Science Foundation (NSF) grants DMS-2014928 and DMS-2310881.

REFERENCES

- [1] J. Agterberg, Z. Lubberts, and J. Arroyo, “Joint spectral clustering in multilayer degree-corrected stochastic blockmodels,” *ArXiv: 2212.05053*, 2022.
- [2] J. Agterberg and A. Zhang, “Estimating higher-order mixed memberships via the $\ell_{2,\infty}$ tensor perturbation bound,” *ArXiv: 2212.08642*, 2022.
- [3] E. M. Airoldi, D. M. Blei, S. E. Fienberg, and E. P. Xing, “Mixed membership stochastic blockmodels,” *J. Mach. Learn. Res.*, vol. 9, pp. 1981–2014, Jun. 2008.
- [4] J. Arroyo, A. Athreya, J. Cape, G. Chen, C. E. Priebe, and J. T. Vogelstein, “Inference for multiple heterogeneous networks with a common invariant subspace,” *Journal of Machine Learning Research*, vol. 22, no. 142, pp. 1–49, 2021. [Online]. Available: <http://jmlr.org/papers/v22/19-558.html>
- [5] A. Athreya, D. E. Fishkind, M. Tang, C. E. Priebe, Y. Park, J. T. Vogelstein, K. Levin, V. Lyzinski, Y. Qin, and D. L. Sussman, “Statistical inference on random dot product graphs: a survey,” *Journal of Machine Learning Research*, vol. 18, no. 226, pp. 1–92, 2018. [Online]. Available: <http://jmlr.org/papers/v18/17-448.html>
- [6] A. Athreya, Z. Lubberts, Y. Park, and C. E. Priebe, “Discovering underlying dynamics in time series of networks,” *ArXiv: 2205.06877*, 2022.
- [7] F. Benaych-Georges, C. Bordenave, and A. Knowles, “Spectral radii of sparse random matrices,” *Annales de l’Institut Henri Poincaré, Probabilités et Statistiques*, vol. 56, no. 3, pp. 2141 – 2161, 2020. [Online]. Available: <https://doi.org/10.1214/19-AIHP1033>
- [8] T. T. Cai and A. Zhang, “Rate-optimal perturbation bounds for singular subspaces with applications to high-dimensional statistics,” *The Annals of Statistics*, vol. 46, no. 1, pp. 60 – 89, 2018. [Online]. Available: <https://doi.org/10.1214/17-AOS1541>
- [9] J. Cape, M. Tang, and C. E. Priebe, “The two-to-infinity norm and singular subspace geometry with applications to high-dimensional statistics,” *The Annals of Statistics*, vol. 47, no. 5, pp. 2405 – 2439, 2019. [Online]. Available: <https://doi.org/10.1214/18-AOS1752>
- [10] J. Cheng, T. Li, E. Levina, and J. Zhu, “High-dimensional mixed graphical models,” *Journal of Computational and Graphical Statistics*, vol. 26, no. 2, pp. 367–378, 2017.
- [11] E. C. Chi, B. J. Gaines, W. W. Sun, H. Zhou, and J. Yang, “Provable convex co-clustering of tensors,” *Journal of Machine Learning Research*, vol. 21, no. 214, pp. 1–58, 2020. [Online]. Available: <http://jmlr.org/papers/v21/18-155.html>
- [12] M. Cucuringu, D. P. G. A., and H. Tyagi, “SPONGE: A generalized eigenproblem for clustering signed networks,” *AISTATS*, 2019.
- [13] J. A. Davis, “Clustering and structural balance in graphs,” *Human relations*, vol. 20, no. 2, pp. 181–187, 1967.
- [14] M. De Domenico, V. Nicosia, A. Arenas, and V. Latora, “Structural reducibility of multilayer networks,” *Nature Communications*, vol. 6, no. 6864, 2015.
- [15] D. Donoho, M. Gavish, and E. Romanov, “ScreeNOT: Exact MSE-optimal singular value thresholding in correlated noise,” *The Annals of Statistics*, vol. 51, no. 1, pp. 122 – 148, 2023. [Online]. Available: <https://doi.org/10.1214/22-AOS2232>
- [16] J. Fan and Y. Fan, “High-dimensional classification using features annealed independence rules,” *The Annals of Statistics*, vol. 36, no. 6, pp. 2605 – 2637, 2008. [Online]. Available: <https://doi.org/10.1214/07-AOS504>
- [17] X. Fan, M. Pensky, F. Yu, and T. Zhang, “Alma: Alternating minimization algorithm for clustering mixture multilayer network,” *Journal of Machine Learning Research*, vol. 23, no. 330, pp. 1–46, 2022. [Online]. Available: <http://jmlr.org/papers/v23/21-0182.html>
- [18] I. Gallagher, A. Jones, A. Bertiger, C. E. Priebe, and P. Rubin-Delanchy, “Spectral embedding of weighted graphs,” *Journal of the American Statistical Association*, vol. 0, no. 0, pp. 1–10, 2023+. [Online]. Available: <https://doi.org/10.1080/01621459.2023.2225239>
- [19] C. Gao, Z. Ma, A. Y. Zhang, and H. H. Zhou, “Achieving optimal misclassification proportion in stochastic block models,” *J. Mach. Learn. Res.*, vol. 18, no. 1, pp. 1980–2024, Jan. 2017.
- [20] —, “Community detection in degree-corrected block models,” *Ann. Statist.*, vol. 46, no. 5, pp. 2153–2185, 10 2018.
- [21] R. Han, Y. Luo, M. Wang, and A. R. Zhang, “Exact clustering in tensor block model: Statistical optimality and computational limit,” *Journal of the Royal Statistical Society Series B*, vol. 84, no. 5, pp. 1666–1698, November 2022.
- [22] F. Harary, “On the notion of balance of a signed graph,” *Michigan Mathematical Journal*, vol. 2, no. 2, pp. 143 – 146, 1953. [Online]. Available: <https://doi.org/10.1307/mmj/1028989917>
- [23] J. Jin, “A sharp nmf result with applications in network modeling,” in *Advances in Neural Information Processing Systems 35*. Curran Associates, Inc., 2022.
- [24] J. Jin and T.-K. Huang, “Sharp results for niep and nmf,” *Unpublished manuscript*, 2024. [Online]. Available: <https://openreview.net/forum?id=z8q8kBxC5H>
- [25] B.-Y. Jing, T. Li, Z. Lyu, and D. Xia, “Community detection on mixture multilayer networks via regularized tensor decomposition,” *The Annals of Statistics*, vol. 49, no. 6, pp. 3181 – 3205, 2021. [Online]. Available: <https://doi.org/10.1214/21-AOS2079>
- [26] A. Jones and P. Rubin-Delanchy, “The multilayer random dot product graph,” *ArXiv: 2007.10455*, 2020.
- [27] Z. T. Ke and J. Wang, “Optimal network membership estimation under severe degree heterogeneity,” *ArXiv:2204.12087*, 2022.
- [28] M. Kivela, A. Arenas, M. Barthelemy, J. P. Gleeson, Y. Moreno, and M. A. Porter, “Multilayer networks,”

- Journal of Complex Networks*, vol. 2, no. 3, pp. 203–271, 07 2014. [Online]. Available: <https://doi.org/10.1093/comnet/cnu016>
- [29] J. Koo, M. Tang, and M. W. Trosset, “Popularity adjusted block models are generalized random dot product graphs,” *Journal of Computational and Graphical Statistics*, vol. 0, no. 0, pp. 1–14, 2022. [Online]. Available: <https://doi.org/10.1080/10618600.2022.2081576>
- [30] C. M. Le, E. Levina, and R. Vershynin, *Concentration of random graphs and application to community detection*. ICM, 2018, pp. 2925–2943.
- [31] J. Lei and K. Z. Lin, “Bias-adjusted spectral clustering in multi-layer stochastic block models,” *Journal of the American Statistical Association*, vol. 118, no. 544, pp. 2433–2445, 2023.
- [32] J. Lei and A. Rinaldo, “Consistency of spectral clustering in stochastic block models,” *Ann. Statist.*, vol. 43, no. 1, pp. 215–237, 02 2015.
- [33] Y. Luo, G. Raskutti, M. Yuan, and A. R. Zhang, “A sharp blockwise tensor perturbation bound for orthogonal iteration,” *Journal of Machine Learning Research*, vol. 22, no. 179, pp. 1–48, 2021. [Online]. Available: <http://jmlr.org/papers/v22/20-919.html>
- [34] M. Noroozi, R. Rimal, and M. Pensky, “Estimation and clustering in popularity adjusted block model,” *Journal of The Royal Statistical Society Series B-statistical Methodology*, vol. 83, pp. 293–317, 2021.
- [35] M. Noroozi and M. Pensky, “Sparse subspace clustering in diverse multiplex network model,” *Journal of Multivariate Analysis*, vol. 203, p. #105333, 2024. [Online]. Available: <https://www.sciencedirect.com/science/article/pii/S0047259X2400040X>
- [36] M. Pensky, “Davis- kahan theorem in the two-to-infinity norm and its application to perfect clustering,” *ArXiv:2411.11728*, 2024.
- [37] M. Pensky and Y. Wang, “Clustering of diverse multiplex networks,” *IEEE Transactions on Network Science and Engineering*, vol. 11, no. 4, pp. 3441–3454, 2024.
- [38] P. Rubin-Delanchy, J. Cape, M. Tang, and C. E. Priebe, “A Statistical Interpretation of Spectral Embedding: The Generalised Random Dot Product Graph,” *Journal of the Royal Statistical Society Series B: Statistical Methodology*, vol. 84, no. 4, pp. 1446–1473, 06 2022. [Online]. Available: <https://doi.org/10.1111/rssb.12509>
- [39] O. Sporns, “Graph theory methods: applications in brain networks,” *Dialogues in Clinical Neuroscience*, vol. 20, no. 2, pp. 111–121, 2018.
- [40] L. Sun, R. Patel, J. Liu, K. Chen, T. Wu, J. Li, E. M. Reiman, and J. Ye, “Mining brain region connectivity for alzheimer’s disease study via sparse inverse covariance estimation,” in *Knowledge Discovery and Data Mining*, 2009. [Online]. Available: <https://api.semanticscholar.org/CorpusID:7857678>
- [41] J. A. Tropp, “User-friendly tail bounds for sums of random matrices,” *Foundations of Computational Mathematics*, vol. 12, no. 4, pp. 389–434, 2011.
- [42] J. M. Tyszk, D. P. Kennedy, L. K. Paul, and R. Adolphs, “Largely typical patterns of resting-state functional connectivity in high-functioning adults with autism,” *Cerebral Cortex*, vol. 24, no. 7, pp. 1894–1905, Jul 2014.
- [43] M. J. Wainwright, *High-Dimensional Statistics: A Non-Asymptotic Viewpoint*, ser. Cambridge Series in Statistical and Probabilistic Mathematics. Cambridge University Press, 2019.
- [44] Y. Yu, T. Wang, and R. J. Samworth, “A useful variant of the davis-kahan theorem for statisticians,” *Biometrika*, vol. 102, no. 2, pp. 315–323, 04 2014. [Online]. Available: <https://doi.org/10.1093/biomet/asv008>
- [45] A. Zhang and D. Xia, “Tensor svd: Statistical and computational limits,” *IEEE Transactions on Information Theory*, vol. 64, no. 11, pp. 7311–7338, 2018.
- [46] R. Zheng and M. Tang, “Limit results for distributed estimation of invariant subspaces in multiple networks inference and pca,” *ArXiv: 2206.04306*, 2022.



Marianna Pensky is a Professor with the Department of Mathematics, University of Central Florida. She is a Fellow of the Institute of Mathematical Statistics and a Fellow of the American Statistical Association. She is also an executive editor of the *Journal of the Statistical Planning and Inference*.